MiReCOL Mitigation and Remediation of CO_2 Leakage

Project no.:
608608

Project acronym:
MiReCOL

Project title:
Mitigation and remediation of leakage from geological storage

Collaborative Project

Start date of project: 2014-03-01
Duration: 3 years

D5.1

Report to partners justifying the choice of models

(Remediation scenarios linked to CO_2 migration through faults and fractures)

Revision: 5

Organisation name of lead contractor for this deliverable:
IFPEN

Project co-funded by the European Commission within the Seventh Framework Programme		
Dissemination Level		
PU	Public	X
PP	Restricted to other programme participants (including the Commission Services)	
RE	Restricted to a group specified by the consortium (including the Commission Services)	
CO	Confidential , only for members of the consortium (including the Commission Services)	

Deliverable number:	D5.1
Deliverable name:	Report to partners justifying the choice of models (Remediation scenarios linked to CO_2 migration through faults and fractures)
Work package:	WP 5: Remediation linked to transport properties of faults and fracture networks
Lead contractor:	IFPEN

Status of deliverable		
Action	**By**	**Date**
Submitted (Author(s))	B. Orlic	01.09.2014.
	A. Lavrov	22.08.2014
	D. Karas	01.09.2014.
	A. Busch	24.10.2014.
Verified (WP-leader)	B. Orlic	06.12.2014.
Approved (SP-leader)	M. Fleury	10.12.2014.

Author(s)		
Name	**Organisation**	**E-mail**
B. Orlic	TNO	bogdan.orlic@tno.nl
A. Lavrov	SINTEF	alexandre.lavrov@sintef.no
A. Busch	SHELL	andreas.busch@shell.com
D. Karas	NIS	dusan.karas@nis.eu

Public abstract

The MiReCOL project investigates existing and new techniques for remediation and mitigation of leakage from geological CO_2 storage. Assessment of potential leakage through faults and fractured caprocks is of primary concern for geological CO_2 storage sites. Faults and fracture networks can act either as permeability barriers or preferential pathways for fluid flow, depending on the infill and the stresses acting on them. The state of stress is, however, not constant but will change on geological and engineering (production/injection) time scales. Hence, faults and fractures can be open and conductive at some time and closed and non-conductive at other times. This study describes remediation scenarios linked to CO_2 migration through faults and fractures and the methods that will be used in follow-up studies to investigate the feasibility of these remediation scenarios by means of numerical simulations.

Because most fractures are stress-sensitive, we investigate the feasibility of modifying the stress field to decrease the leakage rate through faults and fractures. In this study, the effect of the in-situ stress regime on possible fracture and fault reactivation scenarios has been qualitatively analysed for two kinds of CO_2 storage: deep saline reservoirs; and depleted oil and gas reservoirs. Literature review was performed to summarise the current knowledge on fracture closure laws. In the follow-up study, the effect of stresses on fracture permeability under normal or shear deformation will be quantitatively studied in detail using a hydro-mechanically coupled numerical framework. Closure laws derived in this study will thereupon be used to perform numerical simulations of realistic leakage scenarios through the caprock. This will be done by means of prototypical models, or for a real field case (e.g. Bečej field in Serbia), if enough input

Copyright © MiReCOL Consortium 2014-2017

data becomes available for the latter. The effect of changing stress field under different injection schedules will be specifically addressed for different tectonic regimes (extensional, compressional, strike-slip).

Another remediation scenario considers mitigation of leakage by diverting CO_2 to nearby reservoir compartments in the storage reservoir. This scenario requires creating a pathway for fluid migration between the injected, leaky compartment and neighbouring compartments, as the injected and neighbouring compartments are originally not connected. A geological setting suitable to investigate the feasibility of remediation by flow diversion comprises a compartmentalized gas reservoir or aquifer. Such structural settings are quite common: e.g. the depleted P18-4 gas reservoir, planned to be used for CO_2 storage in the Rotterdam Capture and Storage Demonstration Project (ROAD), is separated by a sealing fault from the neighbouring P15 depleted gas field. Another example relevant for CO_2 storage in both depleted gas fields and aquifers, are the Rotliegendes reservoir rocks, which are compartmentalized throughout north-western Europe. The feasibility of remediation by flow diversion will be tested in a follow-up study; first on a generic model with two reservoir compartments separated by a fault. In the subsequent phase a realistic reservoir model will be used.

TABLE OF CONTENTS

1 INTRODUCTION AND OBJECTIVES 2

2 MODIFYING THE STRESS FIELD TO DECREASE LEAKAGE RATES 2

2.1 State-of-the-art review of CO_2 migration rates and stress conditions 3

2.1.1 Relevant events at storage sites 3

2.1.2 Stress alteration under injection into an undepleted aquifer 4

2.1.3 Stress alteration under injection into a depleted reservoir 7

2.1.4 Effect of stress alteration on fractures and faults in reservoir and caprock 10

2.1.5 Rock fractures and their role in possible leakage of CO_2 11

2.1.6 Model requirements and description of the CO_2 migration scenarios 18

2.1.7 Concluding remarks 23

3 REMEDIATION OF LEAKAGE BY DIVERSION OF CO_2 TO NEARBY RESERVOIR COMPARTMENTS 24

3.1 State-of-the-art review of fault sealing behaviour and hydraulic fracturing in the oil and gas industry 24

3.1.1 Faults 24

3.1.2 Hydraulic fracturing 29

3.1.3 Model requirements and description of the CO_2 mitigation scenarios 35

3.1.4 Concluding remarks 38

4 REFERENCES 39

Copyright © MiReCOL Consortium 2014-2017

1 INTRODUCTION AND OBJECTIVES

The MiReCOL project investigates existing and new techniques for remediation and mitigation of leakage from geological CO_2 storage sites. The present study investigates remediation options linked to transport properties of faults and fracture networks. Fractured caprocks and faults intersecting the caprock are of primary concern as they can act as conduits for CO_2 migration out of the storage reservoir. Faults and fractures can act either as permeability barriers or preferential pathways for fluid flow, depending on their infill and the stresses acting on them. As the state of stress changes during geological history, reservoir production and injection operations, faults and fractures can open and become conductive at some time, or close and become non-conductive at other times.

The main objectives of the research are as follows:

- Review state of the art techniques for assessing leakage rates in faults and fracture networks; describe the possible leakage scenarios and the controlling factors; describe the modelling approaches that will be used in follow-up studies to investigate the feasibility of proposed remediation scenarios.
- Evaluate the impact on leakage rates of changing stress field by decreasing reservoir pressure.
- Test an original approach consisting of transferring CO_2 to another compartment originally unconnected to the storage compartment.

The present study describes remediation scenarios linked to CO_2 migration through faults and fractures. Literature study was performed to summarise the current knowledge on stress-dependent permeability, fracture closure laws, hydro-mechanical behaviour of faults and hydraulic fracturing practices in the oil and gas industry. Subsequently, the methods and approaches are described that will be used in follow-up studies to investigate the feasibility of the proposed remediation scenarios by means of numerical simulations.

2 MODIFYING THE STRESS FIELD TO DECREASE LEAKAGE RATES

The flow rates through fracture systems and faults are usually stress-dependent. If a leak through a fractured caprock or a fault is detected during CO_2 injection, the pressure in the reservoir can be relieved. The pressure change in the reservoir will affect the stress state not only in the reservoir rock, but also in the caprock, surrounding formations and nearby faults. As a consequence, the leakage rates controlled by fractures and faults will also be affected. In this chapter we investigate the feasibility of decreasing the leakage rates controlled by faults and fractures by manipulating the pressure field in the reservoir.

Copyright © MiReCOL Consortium 2014-2017

2.1 State-of-the-art review of CO_2 migration rates and stress conditions

2.1.1 Relevant events at storage sites

Underground storage of CO_2 requires a good understanding of CO_2 trapping and migration in subsurface. Natural analogues of CO_2 storage sites may contribute to such understanding, especially with regard to long-term effects since the lifetime of such sites is significantly longer than what ongoing engineered CO_2 pilot projects can offer. There are usually considered three possible types of leakage scenarios in natural CO_2 sites (Fessenden *et al.*, 2009):

- focused leakage, e.g. in the form of a geyser, which can be considered as analogue to a leaking well in an engineered site;
- diffuse leakage, through a fracture system leading towards but not reaching the surface, which can be considered as analogue to a leakage through a fracture / fault system in caprock of an engineered storage site;
- no leakage.

In practice, the "no leakage" situation might be difficult to achieve in long term. Very slow seepage through porous matrix may occur in a very long term even for a rock with the lowest permeability.

The term 'diffuse leakage' in the above list is not related to the mechanism, i.e. diffusion or viscous flow, but rather to the appearance of the leak in space and time. 'Diffuse leakage' can thus be due to either diffusion or viscous flow (or both). Likewise, 'focused' leakage' can be caused by different mechanisms, e.g. a reactivated fault or a gas chimney.

An example of focused leakage from a natural site is the Crystal Geyser in Utah created by a well drilled into a natural-CO_2-bearing formation. The geyser has an average CO_2 release rate of 40-50 t/day (Friedman, 2007).

An example of diffuse leakage can be found e.g. in California, at the base of Mammoth Mountain, with CO_2 flux of 7.5 kg/(m^2/day) over an area of 5-10 ha (Fessenden *et al.*, 2009). In the case of diffuse leakage, CO_2 typically spreads horizontally through a system of connected fractures and faults. This particular site started to leak in 1989 after a series of seismic events that supposedly opened up fractures and activated faults.

An example of a natural CO_2 site with no detectable leakage is Bravo Dome in the US (Fessenden *et al.*, 2009).

It was emphasized by Fessenden *et al.* (2009) that "natural analogues can greatly help… since they provide information about the long term fate of CO_2 in a natural system". Extrapolation of results from a leaking or not leaking natural site onto engineered storage sites calls for a closer look at possible similarities and differences in stress variation and fracture/fault dynamics at natural and engineered CO_2 storage sites.

Leakage scenarios during underground storage of CO_2 are often classified into two categories: (1) abrupt leakage caused by a well failure; (2) gradual and diffuse leakage through faults, fractures or wells (Metz *et al.*, 2005). The focus in this Section is on potential leakage through natural or induced fractures, and geological faults.

Copyright © MiReCOL Consortium 2014-2017

It should be noted that engineered storage sites, from stress history point of view, can belong to one of two types:

- depleted oil and gas reservoirs;
- deep saline (undepleted) aquifers.

Stress changes during production of oil and gas have been studied in reservoir geomechanics for the last 20 years (Fjær *et al.*, 2008; Segall and Fitzgerald, 1998; Zoback and Zinke, 2002). Stress dynamics during depletion of an oil reservoir can be briefly summarized as follows, assuming pore pressure only changes inside the reservoir, and the stiffness of the reservoir is not much different from those of the over-, under- and sideburden (Fjær *et al.*, 2008; Segall and Fitzgerald, 1998; Zoback and Zinke, 2002).

- **In the reservoir**: The total vertical stress may become somewhat less compressive due to arching effect. The effective vertical stress becomes more compressive. The total horizontal stress becomes less compressive. The effective horizontal stress becomes more compressive; its change however is smaller than the change in the vertical effective stress. The above stress changes typically promote normal faulting in the reservoir if the overall in-situ stress regime is extensional. They also promote closure of pre-existing vertical fractures in the reservoir.
- **In the overburden**: The vertical stress (total or effective) is unchanged or becomes less compressive due to the effects of the Earth surface. The horizontal stress (total or effective) becomes more compressive. These stress changes may promote reverse faulting if the initial in-situ stress regime was compressional. They also promote closing of vertical fractures.

Field observations at Valhall and Ekofisk fields suggest that normal faulting is indeed promoted in the reservoir during depletion (Zoback and Zinke, 2002). Caution should however be exercised when applying the above qualitative picture for specific fields since it is valid for a perfectly elastic isotropic case with no elastic contrast between the reservoir and the surroundings. Effects of elastic contrast are very significant, as is effects of tilt – so the in situ stress paths may be quite different. It needs to be estimated from case to case using e.g. coupled geomechanical simulations.

2.1.2 Stress alteration under injection into an undepleted aquifer

If CO_2 is injected into a deep saline aquifer surrounded by low-permeability rocks, and the reservoir has not been previously depleted, the stress dynamics will be opposite to that under depletion. Namely:

- **In the reservoir**: The total vertical stress may become somewhat more compressive. The effective vertical stress becomes less compressive. The total horizontal stress becomes more compressive. The effective horizontal stress becomes less compressive; its change however is smaller than the change in the vertical effective stress.

Copyright © MiReCOL Consortium 2014-2017

- **In the overburden**: The vertical stress (total or effective) is unchanged or becomes more compressive due to the effects of the Earth surface. The horizontal stress (total or effective) becomes less compressive.

Here, again, it has been assumed that pore pressure only changes inside the reservoir, and the stiffness of the reservoir is not much different from those of the over-, under- and sideburden. In reality, the cap rock is in undrained state and is typically represented by plastic and anisotropic shale, with mechanical properties different from the reservoir rock. Under such conditions, the pore pressure in the cap rock may change instantly albeit there is no flow, provided the mean stress changes.

The above stress changes will have different implications in different tectonic environments. This is illustrated by Mohr circles in Figure 2.1, Figure 2.2 and Figure 2.3 for extensional (normal faulting), compressional (reverse faulting) and strike-slip regimes, respectively. Note that the stress changes in the overburden appear inconsistent with results of (Vilarrasa, 2014). The reason is that a reservoir of infinite horizontal extension was analysed in the latter. We are considering a reservoir having finite dimensions in all directions.

The reservoir part of Figure 2.1 can be found e.g. in Magri *et al.* (2013) for a specific field case.

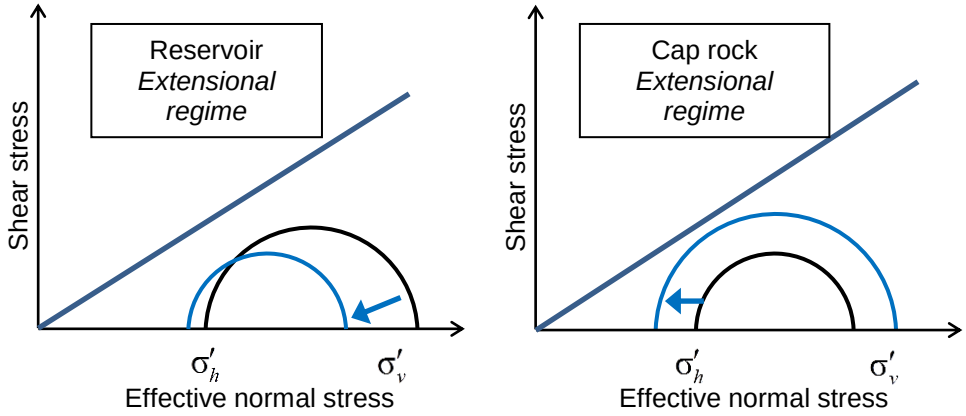

Figure 2.1 Schematic illustration of effective stress alterations in reservoir and overburden (caprock) during injection into an undepleted deep saline aquifer of finite horizontal and vertical dimensions. Extensional (normal faulting) in-situ stress regime is assumed. Pore pressure is assumed to remain constant outside the reservoir. Mechanical properties of the reservoir and surrounding rocks are assumed to be the same. Black Mohr circle: before injection. Blue Mohr circle: during injection (pore pressure increase in the reservoir). Blue arrow indicates possible change of the Mohr circle caused by injection. Subscripts 'v' and 'h' refer to the vertical and minimum horizontal stresses, respectively.

Copyright © MiReCOL Consortium 2014-2017

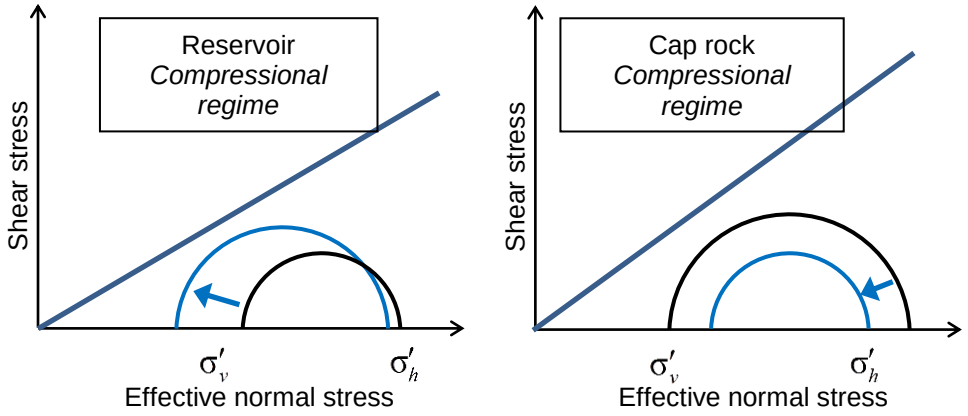

Figure 2.2 Schematic illustration of effective stress alterations in reservoir and overburden (caprock) during injection into an undepleted deep saline aquifer of finite horizontal and vertical dimensions. Compressional (reverse faulting) in-situ stress regime is assumed. Pore pressure is assumed to remain constant outside the reservoir. Mechanical properties of the reservoir and surrounding rocks are assumed to be the same. Black Mohr circle: before injection. Blue Mohr circle: during injection (pore pressure increase in the reservoir). Blue arrow indicates possible change of the Mohr circle caused by injection. Subscripts 'v' and 'h' refer to the vertical and minimum horizontal stresses, respectively.

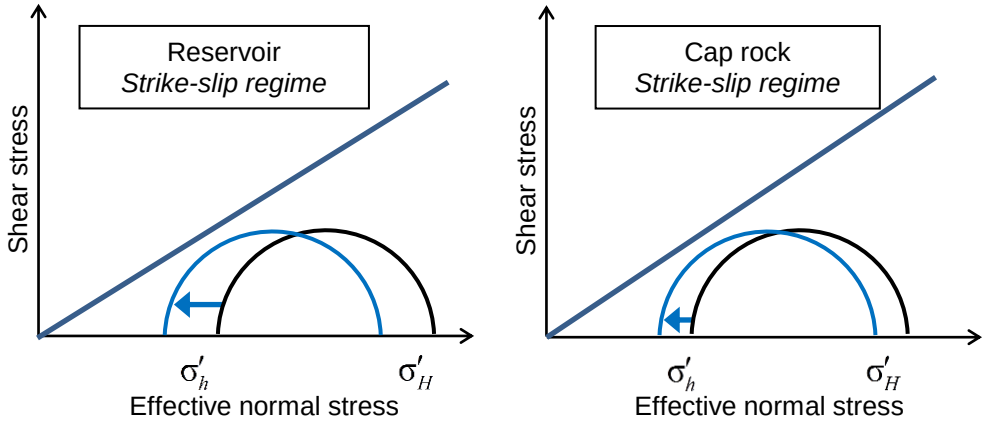

Figure 2.3 Schematic illustration of effective stress alterations in reservoir and overburden (caprock) during injection into an undepleted deep saline aquifer of finite horizontal and vertical dimensions. Strike-slip in-situ stress regime is assumed. Pore pressure is assumed to remain constant outside the reservoir. Mechanical properties of the reservoir and surrounding rocks are assumed to be the same. Black Mohr circle: before injection. Blue Mohr circle: during injection (pore pressure increase in the reservoir). Blue arrow indicates possible change of the Mohr circle caused by injection. Subscripts 'H' and 'h' refer to the maximum and minimum horizontal stresses, respectively.

Copyright © MiReCOL Consortium 2014-2017

2.1.3 Stress alteration under injection into a depleted reservoir

Injection of CO_2 into geological formations increases the pore pressure. As a result, the effective normal stress on pre-existing faults and shear fractures is generally reduced. This, in turn, reduces frictional resistance on the fracture surfaces, thus facilitating reactivation of faults and shear fractures by slip. In addition, increasing the pore pressure above a certain level may induce hydraulic fracturing in the reservoir that might or might not propagate into the overburden. Finally, injection changes the overall state of stress in and around the reservoir because of poroelastic effects.

An important aspect during injection into depleted reservoirs is the effect of reservoir stress path. Stress path can be defined as the ratio of the increase in the total horizontal stress to the increase in the pore pressure that caused it, $\beta_h = \Delta\sigma_h / \Delta P_p$ or $\beta_H = \Delta\sigma_H / \Delta P_p$. While the stress path during depletion can often be about 0.5-0.8 (Nelson *et al.*, 2005), it can be much smaller, down to almost zero, during subsequent injection into the depleted field (Santarelli *et al.*, 1998). More research on stress path during depletion – reinjection is needed in order to find out how common the abnormally low stress paths reported in the literature are under different tectonic regimes and geological settings.

From geomechanical viewpoint, depletion corresponds to reservoir loading (increase of effective stresses). Subsequent injection into a depleted reservoir corresponds to its unloading. Zero (or low) stress path is believed to be due to plastic deformation created in the reservoir by its loading during depletion. Detrimental role of possibly zero stress path during injection of CO_2 into a depleted field was recognized in a recent publication (Vidal-Gilbert *et al.*, 2010).

Assume that during both depletion and subsequent injection the pore pressure only changes inside the reservoir, and the stiffness of the reservoir is not much different from those of the over-, under- and sideburden. Under these assumptions, stress changes under depletion and injection are illustrated in Figure 2.4, Figure 2.5 and Figure 2.6 for extensional (normal faulting), compressional (reverse faulting) and strike-slip regimes, respectively. The reservoir parts of Figure 2.4 and Figure 2.6 can be found in (Vidal-Gilbert *et al.*, 2010) for a specific field case. Stress changes during depletion are shown by black arrows in these Figures. Two cases are illustrated in each Figure: Stress changes with zero reservoir stress path during injection are shown by yellow arrows. Stress changes with unchanged, original stress path during injection are shown by blue arrows. The latter case corresponds to reversible reservoir deformation during depletion-injection. The stress path in the overburden (caprock) is assumed to be the same under depletion and injection, i.e. no irreversible deformation occurs in the caprock under depletion. Moreover, the stress path in the overburden (caprock) is assumed to be unaffected by possibly zero reservoir stress path. In reality, the latter might not be the case. The stress paths for the minimum and maximum horizontal stresses are assumed to be equal in Figure 2.6 ($\beta_h = \beta_H$).

Non-zero stress path and non-unity Biot effective stress coefficient reduce the risk of fault reactivation in the reservoir in normal and strike-slip regimes (Orlic *et al.*, 2011; Vidal-Gilbert *et al.*, 2010).

Copyright © MiReCOL Consortium 2014-2017

Irreversibility represented by zero (or very low) stress path is expected to have profound effects on the reservoir and caprock integrity. In particular, if normal faults have been reactivated in the reservoir during depletion, they will not be able to return to their initial state during injection because it is not possible to reconstruct the pre-depletion state of stress by simply re-pressurizing the reservoir to the same pressure. In addition, hydraulic conductivity of fractures subject to shear deformation is irreversible (Esaki *et al.*, 1999) and thus may persist even in the case of a sufficiently high stress path, β_h, during injection.

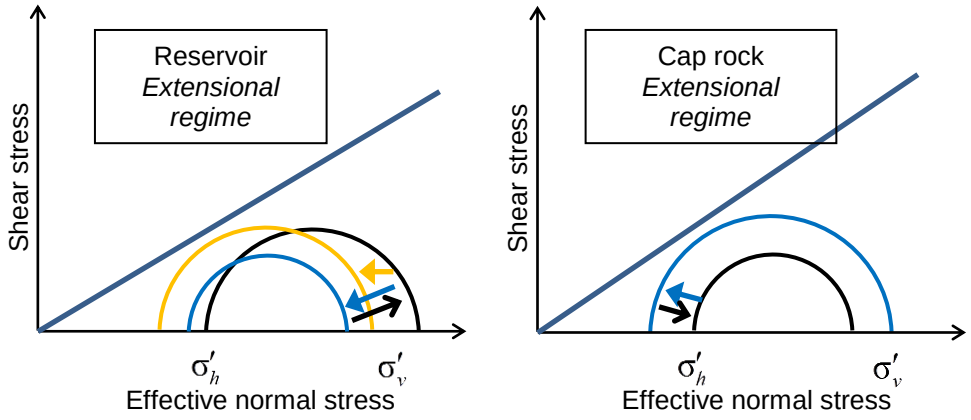

Figure 2.4 Schematic illustration of effective stress alterations in reservoir and overburden (caprock) during injection into a depleted reservoir of finite horizontal and vertical dimensions. Extensional (normal faulting) in-situ stress regime is assumed. Pore pressure is assumed to remain constant outside the reservoir. Mechanical properties of the reservoir and surrounding rocks are assumed to be the same. Black Mohr circle: after depletion. Blue Mohr circle: during injection (pore pressure increase in the reservoir), assuming unchanged stress path (reversible deformation). Yellow Mohr circle: during injection (pore pressure increase in the reservoir), assuming zero stress path. Subscripts 'v' and 'h' refer to the vertical and minimum horizontal stresses, respectively.

Copyright © MiReCOL Consortium 2014-2017

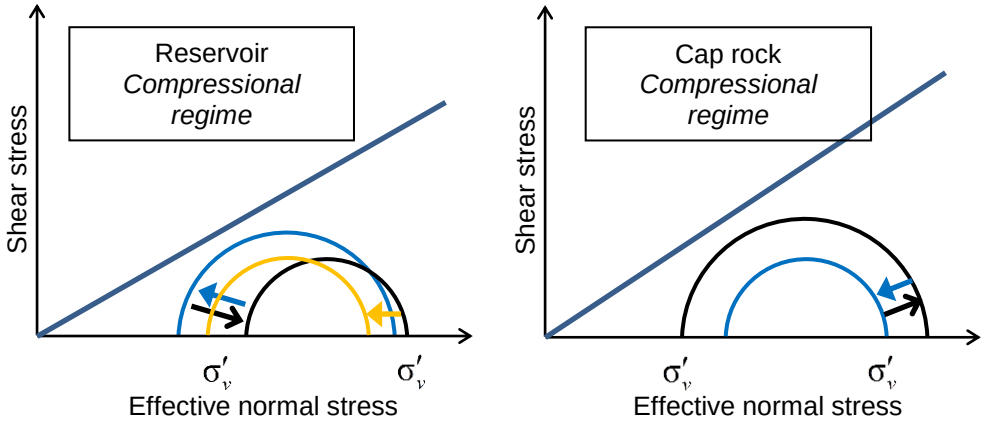

Figure 2.5 Schematic illustration of effective stress alterations in reservoir and overburden (caprock) during injection into a depleted reservoir of finite horizontal and vertical dimensions. Compressional (reverse faulting) in-situ stress regime is assumed. Pore pressure is assumed to remain constant outside the reservoir. Mechanical properties of the reservoir and surrounding rocks are assumed to be the same. Black Mohr circle: after depletion. Blue Mohr circle: during injection (pore pressure increase in the reservoir), assuming unchanged stress path (reversible deformation). Yellow Mohr circle: during injection (pore pressure increase in the reservoir), assuming zero stress path. Subscripts 'v' and 'h' refer to the vertical and minimum horizontal stresses, respectively.

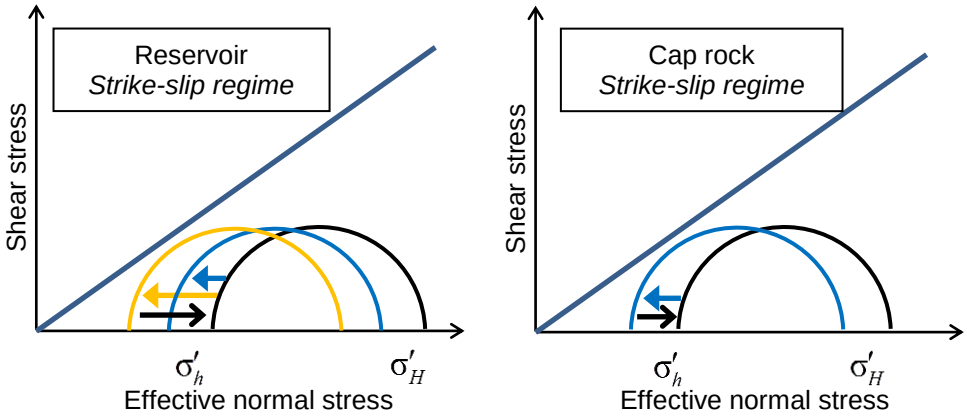

Figure 2.6 Schematic illustration of effective stress alterations in reservoir and overburden (caprock) during injection into a depleted reservoir of finite horizontal and vertical dimensions. Strike-slip in-situ stress regime is assumed. Pore pressure is assumed to remain constant outside the reservoir. Mechanical properties of the reservoir and surrounding rocks are assumed to be the same. Black Mohr circle: after depletion. Blue Mohr circle: during injection (pore pressure increase in the reservoir), assuming unchanged stress path (reversible deformation). Yellow Mohr circle: during injection (pore pressure increase in the reservoir), assuming zero stress path. Subscripts 'H' and 'h' refer to the maximum and minimum horizontal stresses, respectively.

Copyright © MiReCOL Consortium 2014-2017

2.1.4 Effect of stress alteration on fractures and faults in reservoir and caprock.

Stress changes that can be expected during CO_2 injection into a deep saline aquifer or a depleted oil reservoir were summarised above. Due to large variation and heterogeneity in rock properties and complex geological structures, the stress variations can be much more complex in real life. However, our simplified treatment still provides some hints about the geomechanical effects on reservoir and caprock stability during injection. Mechanisms affecting stability can be derived from Figure 2.1 to Figure 2.6 and are summarized in Table 2.1. In addition to the effects listed in Table 2.1, reactivation of shear fractures and faults may enhance permeability in the direction of the intermediate in-situ stress due to the "tubular" effect at shear fracture intersections (Sibson, 1996). This may, consequently, facilitate horizontal spreading of CO_2 under extensional and compressional stress regimes.

It is important to emphasize that possible activation of each of the mechanisms listed in Table 2.1, such as e.g. tensile fractures or thrusts, ultimately depends on mechanical properties of rocks and faults, and on the specific values of pore pressure and stress magnitudes before, during and after injection. The descriptions in Table 2.1 only indicate what can possibly happen, provided e.g. that the fluid pressure becomes high enough or the rock strength is sufficiently small. Also, in real life, the picture can and probably will be complicated by pore pressure diffusion from the reservoir into the surrounding low-permeability rock that was neglected when constructing Figure 2.1 to Figure 2.6. Moreover, even when fracturing occurs, it will not necessarily lead to leakage. For instance, fractures may fail to establish a connected network. Some fractures might close after injection is finished provided that shear displacement was sufficiently small on those fractures. A detailed analysis is required for each specific case in order to assess the risks associated with stress changes and possible fracturing during CO_2 injection.

It should be noted that shear and tensile fractures generated or reactivated in the reservoir might improve the injectivity by reducing the flow resistance (Nelson *et al.*, 2005). However, propagation of such fractures into the caprock may represent a risk factor for caprock integrity (Orlic *et al.*, 2011; Streit and Hillis, 2004). And so may fault reactivation inside the reservoir if the slip displacement propagates into the caprock. In any event, the effect of changing reservoir pressure on the stress state in the caprock is typically smaller than on the stress state in the reservoir itself (Orlic *et al.*, 2011). Therefore fracture and fault reactivation scenarios in the caprock under depletion shown in the last column of Table 2.1 will most likely be able to develop only after the onset of fracture or fault reactivation in the reservoir. Another important contributing factor that should be carefully examined for storage in depleted reservoirs is damage that possibly has been created in the caprock during depletion (Orlic *et al.*, 2011; Streit and Hillis, 2004). This may include fault reactivation, wellbore casing failure or formation of new fractures (Streit and Hillis, 2004).

Copyright © MiReCOL Consortium 2014-2017

Table 2.1 Possible fracturing scenarios during CO_2 injection in different tectonic regimes. 'Pore pressure' in the Table refers to the reservoir pore pressure. Pore pressure in the caprock is assumed to remain unchanged.

Type of storage	Stress regime	Reservoir	Caprock
Deep saline aquifer	Extensional (normal faulting)	Possible opening of subvertical fractures if pore pressure becomes sufficiently high.	Possible reactivation of normal faults and shear fractures. Possible opening of subvertical fractures if pore pressure becomes sufficiently high.
	Compressional (reverse faulting)	Possible reactivation of thrusts and shear fractures. Possible opening of subvertical fractures if pore pressure becomes sufficiently high.	
	Strike-slip	Possible reactivation of strike-slip faults and shear fractures. Possible opening of subvertical fractures if pore pressure becomes sufficiently high.	Possible reactivation of strike-slip faults and shear fractures. Possible opening of subvertical fractures if pore pressure becomes sufficiently high.
Depleted reservoir	Extensional (normal faulting)	Possible reactivation of normal faults if stress path is sufficiently low during injection. Possible opening of subvertical fractures if stress path is sufficiently low compared to its value during depletion, and pore pressure becomes sufficiently high.	Possible reactivation of normal faults after pore pressure becomes sufficiently larger than it was before depletion.
	Compressional (reverse faulting)	Possible reactivation of reverse faults if stress path during injection is sufficiently high (i.e. unchanged with regard to its value during depletion).	
	Strike-slip	Possible reactivation of strike-slip faults and shear fractures if stress path is sufficiently low during injection. Possible opening of subvertical fractures if pore pressure becomes sufficiently high.	Possible reactivation of strike-slip faults and shear fractures becomes sufficiently larger than it was before depletion. Possible opening of subvertical fractures if pore pressure becomes sufficiently high.

2.1.5 Rock fractures and their role in possible leakage of CO_2

One of the main factors controlling possible leakage of CO_2 from underground storage facilities is believed to be flow through fractures and faults, either in the near-well area, or farther away in the caprock (Fessenden *et al.*, 2009; Orlic *et al.*, 2011).

Fractures are present in most rocks. Intergranular microcracks, extensional fractures, joints, shear fractures are all examples of fractures found on different scales. Given the abundance of fractures and faults in the Earth crust, it is important to be able to predict the risk and extent of leakage through fractures and faults at CCS sites. This requires a good understanding of hydro-mechanical behaviour of fractures and faults.

Copyright © MiReCOL Consortium 2014-2017

It should be noted that being able to predict CO_2 flow in natural fractures is important not only because of possible leakage but also because it may influence the injectivity and the storage capacity of the CCS site. Experiments and numerical simulations suggest that CO_2 can bypass the matrix if fractures of sufficient permeability are available in the formation (Oh *et al.*, 2013). This may reduce the matrix storage capacity and the overall storage capacity of the reservoir. It is conceivable that this might also impact plume migration along such fractures and the predictability of it. It is not improbable that channelization through fractures might deliver CO_2 into parts of the reservoir where it is actually not supposed to be, such as e.g. close to faults or abandoned wells.

Hydraulic properties of fractures; implications for CCS; concept of hydraulic aperture

Fracture surfaces are rough. In particular, landscapes of natural tensile fracture surfaces are known to exhibit more or less regular structures reflecting their growth process, such as hackle plumes (Bahat *et al.*, 2005). Roughness, contact points and mineral deposits between fracture faces contribute to flow tortuosity which effectively means an increase in flow resistance.

In flow modelling, the fracture conductivity is usually characterized by the so called *hydraulic aperture* which is the aperture of a conduit with smooth parallel plane walls that exhibits the same flow rate under a given pressure gradient as the rough-walled fracture does. The *mechanical aperture* is defined as an average geometric distance between fracture faces. Numerous studies suggest that the hydraulic aperture of rock fractures is smaller than the mechanical aperture, sometimes by a factor of 5-6 (Esaki *et al.*, 1999). It is the hydraulic, not mechanical, aperture, w_h, that controls the flow rate through the fracture.

At low Reynolds numbers, the flow rate, **q**, of a Newtonian fluid in the fracture is given by the "cubic law" (Brown, 1987; Zimmerman *et al.*, 1991):

$$\mathbf{q} = -\frac{w_h^3}{12\eta}\nabla P \qquad \text{(Eq. 2.1)}$$

where P is the fluid pressure; η is the dynamic viscosity of the fluid.

Fracture initiation, propagation and reopening in CO_2 storage

Natural and induced fractures represent potential escape paths for fluids injected into geological formations. In particular, faults and fractures are found to be the most common leakage pathway in natural CO_2 leakage incidents reviewed by (Lewicki *et al.*, 2007).

Fractures can be natural (pre-existing), or be created by pressurization during injection, or be due to damage incurred during fault reactivation. How much a particular fracture contributes to leakage depends on its morphology, connectivity to other fractures, orientation with respect to in-situ stresses etc. These factors are discussed further in this Section.

Copyright © MiReCOL Consortium 2014-2017

Behaviour of natural or induced fractures during CO_2 injection into subsurface can be illustrated by means of the extended leak-off test (XLOT) used in oil and gas industry to evaluate the minimum in-situ stress. During this test, fluid is injected into the formation until the formation fractures, and beyond. A typical pressure *vs* time curve obtained in an XLOT is schematically shown in Figure 2.7. A detailed coverage of XLOT can be found e.g. in (Fjær *et al.*, 2008; Raaen *et al.*, 2006).

After the first injection and the subsequent shut-in and bleed-off (flow-back) phases, a repeat cycle of the test is performed. This repeat cycle, on the right in Figure 2.7, can be used to illustrate the behaviour of a pressurized natural fracture located in the near-well area or farther away from the injector. The first injection cycle, on the left in Figure 2.7, is illustrative of induced fractures in the near-well area.

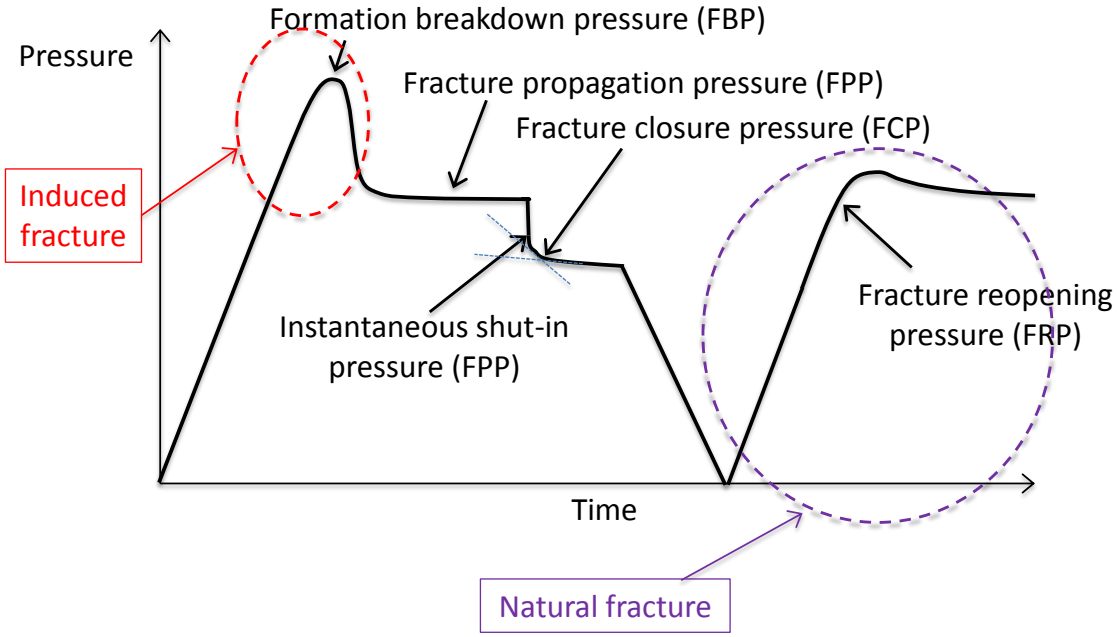

Figure 2.7 Injection pressure vs time in an extended leak-off test (XLOT). Origin corresponds to the pressure equal to the pore pressure (formation fluid pressure).

Leakage through natural fractures and faults

Three flow situations can be conceived, depending on the fluid pressure at the entry point into the fracture, P, relative to the formation fluid pressure, P_p, and the in-situ stresses.

$P = P_p$

The fracture is hydraulically closed in this case. There is hydraulic equilibrium, i.e. there is no hydraulic gradient between the entry point into the fracture and the rest of the fracture. There is therefore no flow. "Entry point" here means e.g. the spot where the injection wellbore intersects the fracture.

Copyright © MiReCOL Consortium 2014-2017

$P_p < P < P_{FRP}$

When the fluid pressure at the point of entry into the fracture, P, exceeds the formation pore pressure, P_p, but is below the fracture re-opening pressure, P_{FRP} (Figure 2.8), the fracture is "closed", but only in the sense that the opposing fracture faces touch each other at asperities. There is a hydraulic gradient inside the fracture. If there were no asperities, i.e. no roughness, the fracture would have zero mechanical and hydraulic aperture, and there would be no flow. However, due to roughness, the fracture is hydraulically opened albeit its hydraulic aperture is significantly smaller than it would be if the fracture faces had been kept apart. Flow is therefore possible although contact spots increase the flow tortuosity and thereby reduce the hydraulic aperture. CO_2 should be able to flow through the fracture under such conditions, albeit its flow rate, being proportional to w_h^3, would be much smaller than in the case of an open fracture ($P > P_{FRP}$) considered below.

$P > P_{FRP}$

When the fluid pressure inside the fracture, P, exceeds the fracture re-opening pressure, the fracture opens up, i.e. asperities on the opposite sides are not in contact any more. As the fracture opens up, its hydraulic aperture increases, and, as Eq.(3.1) shows, it has a dramatic impact on the fracture conductivity. Under such conditions, supercritical CO_2 ($scCO_2$) will eventually be able to flow in the fracture as it becomes sufficiently wide.

In addition, if the natural fracture has a limited extent, and the fluid pressure is increased so as to pass the peak in the repeat cycle (Figure 2.7), the fracture may start propagating (see plateau in the rightmost part of Figure 2.7). Whether such scenario is realistic is an open question.

The scenarios for CO_2 flow in fractures described above are summarized in Figure 2.8.

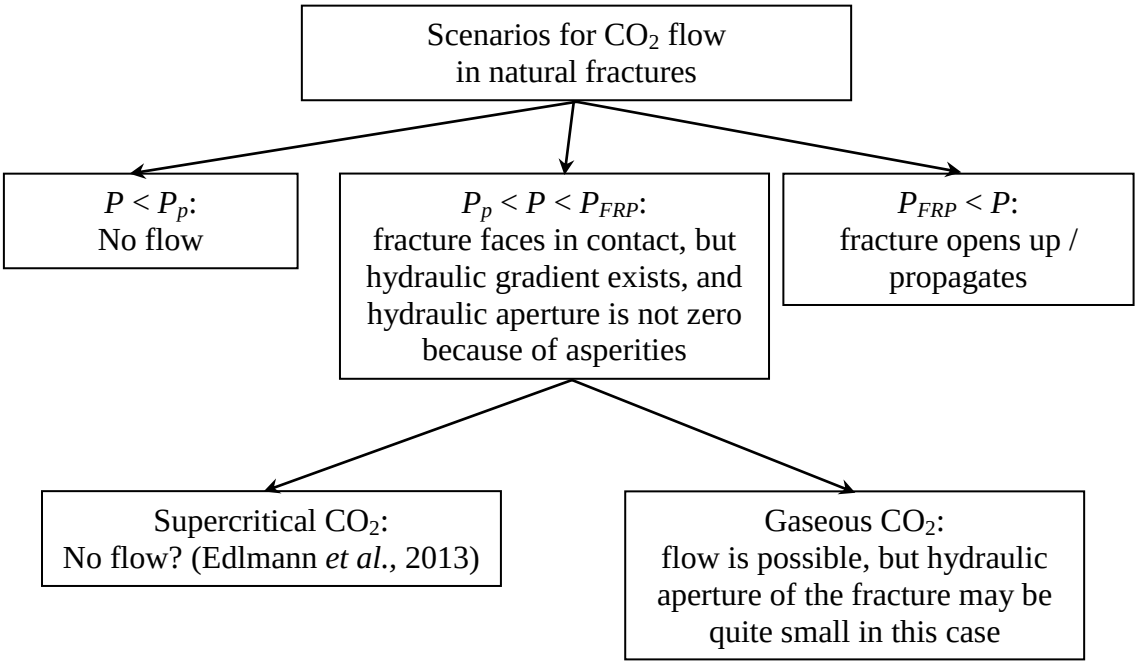

Figure 2.8 Scenarios for CO_2 flow in natural fractures.

Copyright © MiReCOL Consortium 2014-2017

Experimental data on CO_2 flow in fractures

Only few experimental studies on flow of gaseous or supercritical CO_2 in rock fractures have been published.

Edlmann *et al.* (2013) reported that supercritical CO_2 could not flow in closed fractures in their laboratory experiments. Gaseous CO_2 (gCO_2), on the other hand, could flow in the same fractures and under the same pressure gradient. The inability of scCO2 to flow in closed fractures was not supported by experiments of (Oh *et al.*, 2013). In any event, the experiments by Edlmann *et al.* (2013) indicate that fracture permeability to $scCO_2$ can be considerably smaller than to gCO_2.

Oh *et al.* (2013) performed laboratory experiments on fracture flow of $scCO_2$, supported by numerical simulations. The specimen contained one throughgoing artificial fracture. At low injection rates, the CO_2 flow was only through the fracture. As the injection rate was increased, flow through the matrix started, but was considerably slower than in a specimen that did not contain a fracture.

Fracture permeability under stress

Hydraulic aperture of a fracture may change as a result of fracture opening/closing, or due to shear. Moreover, natural fractures, unless they are completely filled with precipitated minerals or gouge, or unless their faces perfectly fit (due to creep on geological time scale, for instance), may have an initial aperture that will contribute to their permeability even if no opening / closing or shear at recent time has occurred. Initial apertures, opening/closing and shear contribute to flow re-distribution during reservoir depletion and re-pressurization under CO_2 injection. They are the most essential components of any numerical model of leakage through fractures. Therefore, the remainder of this Section provides a brief overview of fracture deformation and flow under stress, to be used in the later stages of the project when performing coupled geomechanical simulations of CO_2 flow in fractured rock.

Fracture opening / closing and normal stiffness

If no shear stress is applied on the fracture, and the effective normal stress changes (by changing fluid pressure inside the fracture or by changing the applied normal stress), the fracture will open or close. The fracture faces move in the direction normal to the fracture faces in this case. This is known as mode I in fracture mechanics. The change in the mechanical and, thereby, hydraulic aperture is controlled by the fracture normal stiffness in this case, K_n. The fracture normal stiffness depends on the spatial distribution and the amount of contact spots between the fracture faces (Pyrak-Nolte, 1996). Flow in the fracture depends on the amount and spatial distribution of opened apertures in between the contact spots.

Fracture deformation in mode I is nonlinear: The normal stiffness increases as the applied compressive stress increases (or, equivalently, the fluid pressure inside the fracture decreases) (Pyrak-Nolte, 1996).

Copyright © MiReCOL Consortium 2014-2017

Since both fracture permeability and normal stiffness depend on the amount and distribution of contact spots, there is a relationship between these two properties schematically shown in Figure 2.9.

Figure 2.9 Fracture permeability versus normal stiffness under applied normal stress, after (Pyrak-Nolte, 1996).

Fracture shearing and shear stiffness

When a shear stress is applied to a fracture or a cohesionless fault, the necessary condition for sliding to commence is given by the Coulomb criterion (Nemoto *et al.*, 2008):

$$\tau = \mu(\sigma_n - P) \qquad \text{(Eq. 2.2)}$$

where τ and σ are the shear and normal stress on the fracture surface, respectively; μ is the coefficient of friction, P is the fluid pressure inside the fracture. After the peak in the shear displacement – shear stress curve is reached, the shear stress typically drops to its residual value of about 50% of the peak stress (Figure 2.10) (Esaki *et al.*, 1999). The shear displacement corresponding to the peak was found to be about 1% of the fracture size in laboratory tests (Yeo *et al.*, 1998).

During shear caused by increasing shear stress under a constant normal load, the fracture conductivity increases up until it levels off (Figure 2.11; Esaki *et al.*, 1999). The increase can be 1-2 orders of magnitude. This increase is due to dilatancy caused by surface roughness: Asperities slide over one another, and the fracture opens up (Nemoto *et al.*, 2008).The maximum value of conductivity achievable during the sliding is a function of the maximum height of asperities.

During reverse shearing, the fracture conductivity drops only slightly, and significant conductivity is still maintained when the fracture faces return to their initial position (Figure 2.11). The drop in conductivity during reverse shearing is larger under higher applied normal stress, which was attributed by (Esaki *et al.*, 1999) to fracture plugging by gouge formed by crushing of asperities under elevated normal stress. Irreversible shear deformation of fractures may contribute to their elevated conductivity during the depletion-injection cycle when CO_2 is stored in a depleted reservoir.

Copyright © MiReCOL Consortium 2014-2017

It should be noted that the *experiments* on which Figure 2.10 and Figure 2.11 are based were performed on a hard crystalline rock that does not exhibit swelling and self-sealing. Shear-induced permeability changes can be considerably more complicated in shales due to swelling and smearing of clay minerals under shear displacement (Cuss *et al.*, 2011).

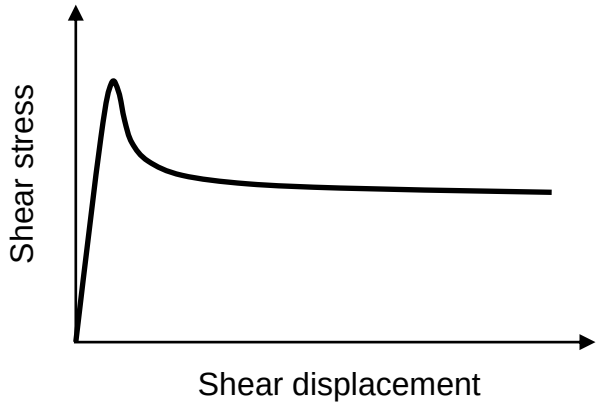

Figure 2.10 Shear stress versus shear displacement during sliding under constant applied normal stress, after (Esaki *et al.*, 1999).

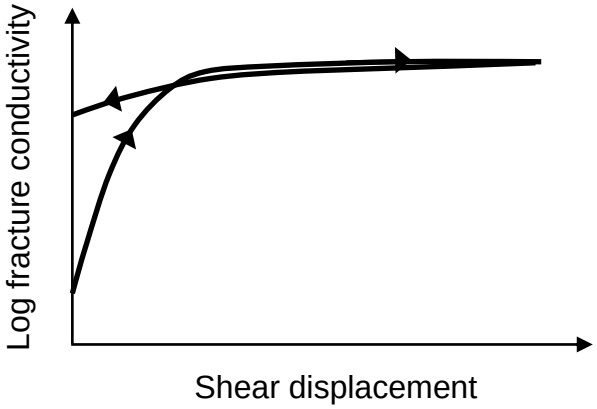

Figure 2.11 Log fracture conductivity vs shear displacement during forward and reverse shearing under constant applied normal stress, after (Esaki *et al.*, 1999).

Key parameters controlling CO_2 leakage through fractures and faults

CO_2 leakage through fractures and faults is mainly controlled by the following factors:

Copyright © MiReCOL Consortium 2014-2017

- in-situ pore pressure (currently existing pressure – as affected by depletion or previous injections);
- locations and dimensions of faults, and their hydraulic and mechanical properties;
- number and orientation of fracture sets;
- spacing of fractures in each set;
- connectivity of the fracture network;
- extent of the fractures and fracture networks in vertical and horizontal directions;
- tectonic regime; magnitude and orientation of in-situ principal stresses (current status – as affected by depletion or previous injections);
- hydraulic aperture of fractures in each set;
- filling of fractures – gouge, mineralization;
- self-sealing potential of fractures (in the long-term perspective)

Moreover, fracture surface roughness and aperture distribution can provide additional information on mechanical and hydraulic behavior of fractures.

2.1.6 Model requirements and description of the CO_2 migration scenarios

The CO_2 mitigation scenarios consider modifying the stress field to decrease the leakage rate.

Model requirements

Since the procedures proposed are quite innovative, much can be learnt from considering, at first, some simplified prototype models of processes that we are dealing with, such as stress-dependent fracture permeability or influence of large-scale stress variations on flow dynamics controlled by fractures and faults. Numerical simulations of a well-documented field case of CO_2 leakage are envisaged at a later stage of the project.

Description of the models selected

Sufficient characterization of the site will be an important criterion for selecting the field case. This should include rock properties, fracture properties (as listed in the section on *Key parameters controlling CO_2 leakage through fractures and faults*), orientation and magnitude of in-situ stresses, fault locations, dimensions and hydro-mechanical properties. In the case of a leaking natural CO_2 site, the data should also include the history of leakage. We intend to focus in particular on the Becej natural CO_2 field (provided by NIS) in which secondary accumulations of CO_2 have been formed in the overburden above the main reservoir. The Becej model is currently under construction and will be described in the subsequent reports. The use of the Becej field implies that enough input data becomes available to us in order to build a representative geomechanical model. In case such data cannot be procured during the project lifetime, we shall perform an extended study of stress field modification effects by means of prototypical models. This will allow us to draw generic conclusions regarding the effects of stress state modification on CO_2 leakage.

Copyright © MiReCOL Consortium 2014-2017

Planned model procedure I

The key parameters controlling migration caused by fractures and faults will be addressed through numerical simulation in this project. Fracture simulation requires that deformation and flow in fractures are first quantified as function of applied stresses (or displacements, normal or shear). Fracture permeability as a function of stresses/displacement then enters as a closure law in the hydro-mechanically coupled simulation framework. Therefore, the following plan of actions can be proposed:

1) Quantify stress-dependent fracture permeability to provide a closure law for coupled geomechanical simulation of leakage through fractures and faults in caprock (Y2014-2015).
2) Establish prototype models of typical expected leakage scenarios in CO_2 storage sites caused by fractures and faults, and taking into account the effect of stress regime on the leakage mechanism as discussed in this report (Y2015).
3) Perform simulations with prototype models (numerical or semi-analytical) (Y2015).
4) Simulate numerically a field case that can be used to investigate the roles and contributions of the leakage mechanisms revealed in prototype models. Pre-requisite for such a simulation is sufficiently detailed characterization of the site, in particular the geomechanical data and the fracture properties listed in Section 3.1.1 (Y2015).
5) Based on the modelling results, provide recommendations on prevention and remediation of leakage under different stress regimes (Y2016).

Quantification of stress-dependent fracture permeability (step 1 in the above plan) will be done by performing simulations of individual fracture deformation (normal or shear) with the finite-element code ABAQUS, taking into account plasticity at contacts between rough fracture surfaces (e.g. Walsh *et al.*, 2013), and possible breakage of asperities. Extended finite-element method (XFEM) available in ABAQUS can be used to model crushing of asperities and nonlinear effects it may cause. Flow in tensile or shear fractures will then be quantified as a function of applied stresses by using the fracture flow code PROPANICA developed at SINTEF (Lavrov, 2013a; b). This modelling workflow is illustrated in Figure 2.12. The computational framework will allow us to establish and test a procedure for providing critically important closure laws for geomechanical simulations of leakage through fractures.

Simulations of leakage in prototypical and real cases (steps 2-5) will be performed by using another fracture modelling framework. Hydro-mechanically coupled fracturing simulator based on the hybrid finite-element / discrete-element fracturing code MDEM developed at SINTEF (Alassi *et al.*, 2011; Lavrov *et al.*, 2014) and the reservoir simulator TOUGH2 developed at Lawrence Berkeley National Laboratory (Pruess *et al.*, 2012) can be used as such framework (Figure 2.13). Other possible choices of the modelling tool will be considered as well.

Copyright © MiReCOL Consortium 2014-2017

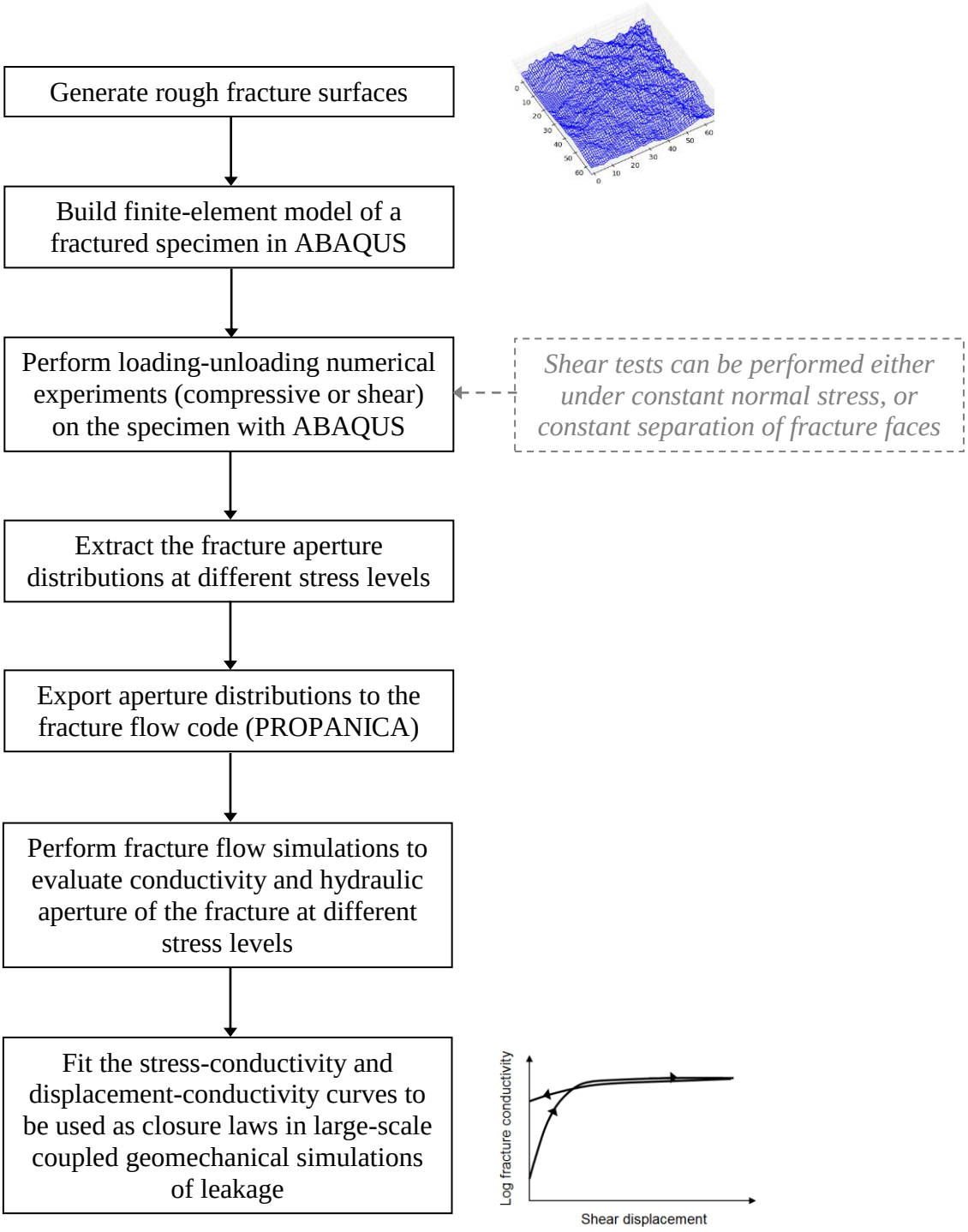

Figure 2.12 Schematic view of the work flow for deriving closure laws for coupled geomechanical simulations of leakages caused by normal and shear fractures.

Copyright © MiReCOL Consortium 2014-2017

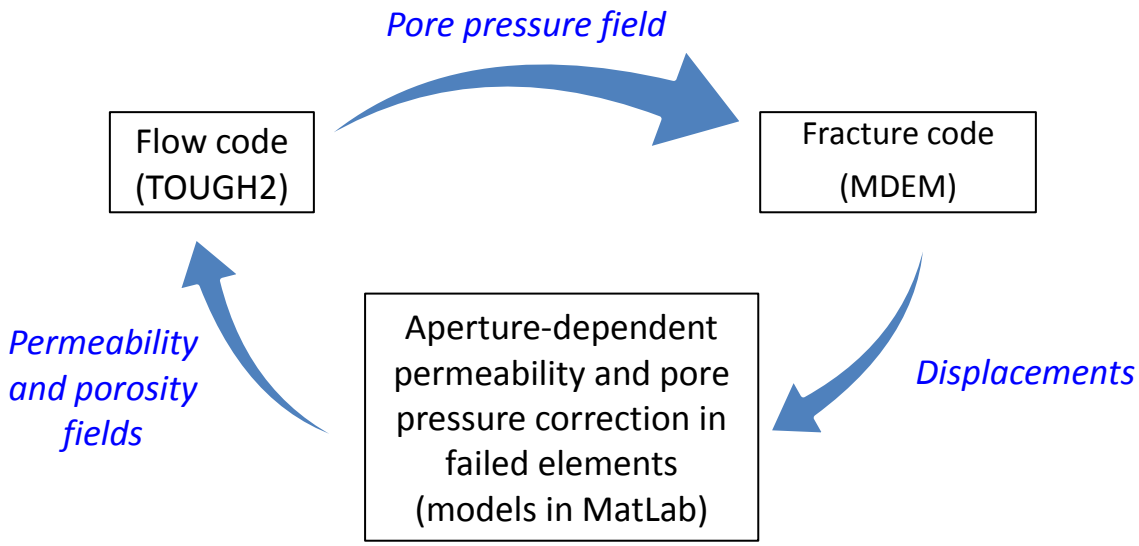

Figure 2.13 Computational flow in hydro-mechanically two-way coupled fracture simulation framework used at SINTEF.

Planned model procedure II

The proposed CO_2 migration scenario is based on the Becej field case. The scenario considers leakage through a channel in the caprock created by a well blowout. This scenario is inspired by a real incident in the Becej field that happened in 1968 (Lakatos *et al.*, 2009).

Gas migration through a channel created by a well blowout is very similar to migration through fractures and faults. A channel consists of a collapsed zone, filled-in by secondary material, and a heavily fractured damaged zone, possibly forming a system of (small) caverns.

The field study of CO_2 leakage will be based on a detailed geological model of the Becej field. Such a model comprises the main gas-saturated reservoir and the complex overburden structure with several shallow aquifers (Figure 2.14).

In the first phase of dynamic modelling, a near-well sector model will be developed, with a leakage channel through the caprock created by a well blowout. The channel connects the main CO_2 reservoir with the shallow overburden, which were initially isolated by the caprock. The near-well model will be based on all the available field information and other reported cases of well blowouts. Such a model will allow calculating the volume of gas that can be released from the reservoir at specific PVT conditions.

Copyright © MiReCOL Consortium 2014-2017

In the second phase of dynamic modelling, a full-field reservoir simulation model of the Becej field will be developed. Geological model of the Becej field in Petrel project format, which contains all available geological and petrophysical information, will be used to develop a full-field simulation model. Suitable methods available in the reservoir simulator will be chosen to adequately represent the geometry and the flow properties of a flow channel (e.g. gridding techniques). The dynamic model will be developed in Eclipse and history-matched with the available pressure data (Figure 2.15).

The full-field model will be used to explore the characteristics and behaviour of a complex flow system consisting of several aquifers in shallow overburden (Figure 2.16). Such a model will also be used to investigate the effectiveness of various mitigation scenarios.

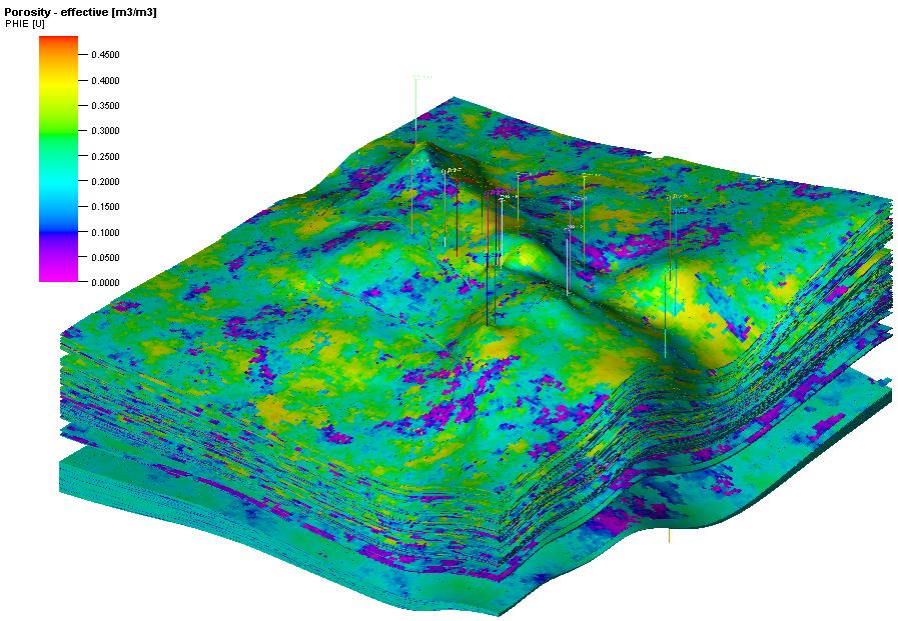

Figure 2.14 Petrel model of the Becej CO_2 field showing permeability distribution in the main reservoir and the overburden with several aquifers.

Copyright © MiReCOL Consortium 2014-2017

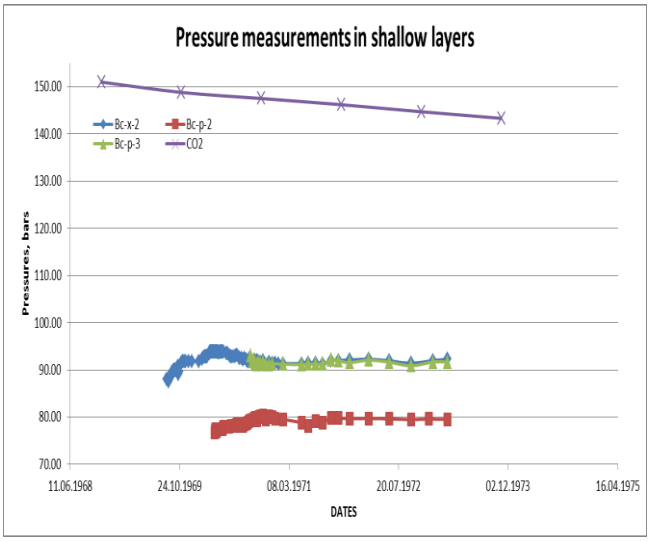

Figure 2.15 Pressure measurements in the shallow layers of the Becej CO_2 field.

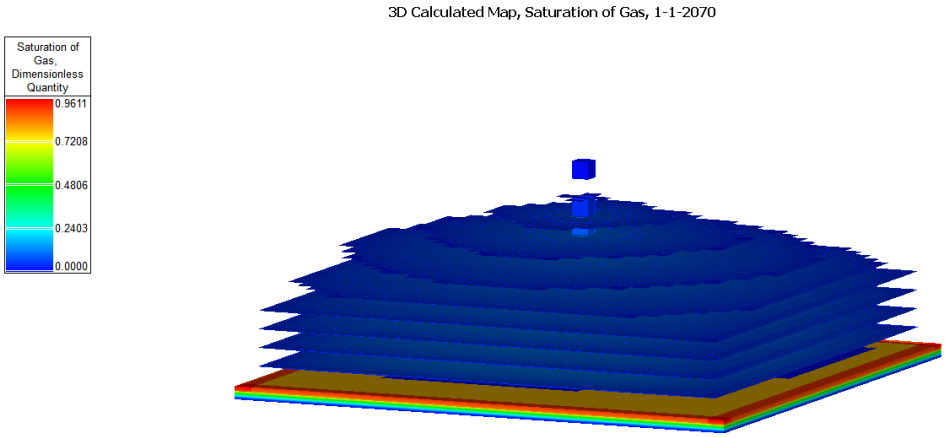

Figure 2.16 Gas saturation due to CO_2 leakage into the overburden from initial reservoir simulations.

2.1.7 Concluding remarks

Leakage through natural or induced fractures in caprock may develop under certain circumstances, under CO_2 injection into either undepleted deep saline or depleted reservoirs. Development of fractures and reactivation of faults is controlled by the reservoir pressure dynamics, rock properties, fracture and fault properties, and by the in-situ stress state. In addition, in the case of depleted reservoirs, fractures created during depletion might contribute to flow. The uncertainty, in the case of depleted reservoirs, is exacerbated by possibly zero or very small stress path, which may result in irreversible behaviour of faults and fractures. In addition, irreversible (hysteretic) behaviour of shear fractures is their inherent property, and may persist even in the case of fully reversible reservoir stress dynamics. This makes numerical modelling of long-term caprock integrity inherently difficult, and requires a good understanding of fracture behaviour under cyclic loading. This issue will be addressed in the project. After the necessary

Copyright © MiReCOL Consortium 2014-2017

stress-permeability closure laws are obtained for some example fractures by means of numerical simulations, hydro-mechanically two-way coupled fracturing simulations under injection will be performed for prototype models as well as for a chosen field case scenario. As a field case scenario, a natural CO_2 analogue site or an engineered site can be used.

3 REMEDIATION OF LEAKAGE BY DIVERSION OF CO_2 TO NEARBY RESERVOIR COMPARTMENTS

Remediation of leakage can be attempted by diversion of CO_2 to a nearby compartment originally unconnected to the main reservoir. Remediation by diversion can be attempted in a compartmentalized gas field or aquifer initially without cross fault communication. Breaching of a fault seal, which separates two neighbouring compartments, can be attempted by multi-stage hydraulic fracturing. Hydraulic fractures represent pathways for transferring CO_2 between two neighbouring, partially juxtaposed reservoir compartments. A realistic reservoir model with a suitable geological and structural setting will be used to test a flow diversion option. Initial simulations will consider a generic model with two compartments separated by a fault. Numerical models will be used to investigate the role of key parameters controlling CO_2 migration between two compartments, such as the number and the flow characteristics of hydraulic fractures.

3.1 State-of-the-art review of fault sealing behaviour and hydraulic fracturing in the oil and gas industry

Literature review considers topics relevant for developing a scenario for remediation of leakage by diversion to nearby compartment. The topics reviewed comprise: fluid flow and geomechanical properties of faults, hydraulic fracturing and the interaction between a hydraulic fracture and a fault.

3.1.1 Faults

Faults have been intensively studied in the petroleum industry as they play an important role in the formation of hydrocarbon accumulations and affect fluid flow during hydrocarbon production. Faults can act as seals and hold the hydrocarbons, or function as conduits and provide a migration route. Faults can be barriers to fluid moving across faults, or can enhance flow in the up-dip direction along faults. Besides in the petroleum industry, faults and fault mechanics have been widely studied in seismology, as the main cause of an earthquake is a sudden movement on a fault (i.e. fault re-activation).

Faults are generally complex zones consisting of a fault core (with sharp fault surfaces, gouge and cataclasite) surrounded by a fault damage zone (with fractures and deformation bands). Typical fault zone structures can have a single core (as shown in Figure 3.1) or multiple cores (e.g. Faulkner *et al.*, 2010). Mechanical and fluid flow properties of fault zones are closely related to the fault zone structure as discussed in detail in review papers by Wibberly *et al.* (2008) and Faulkner *et al.* (2010).

Copyright © MiReCOL Consortium 2014-2017

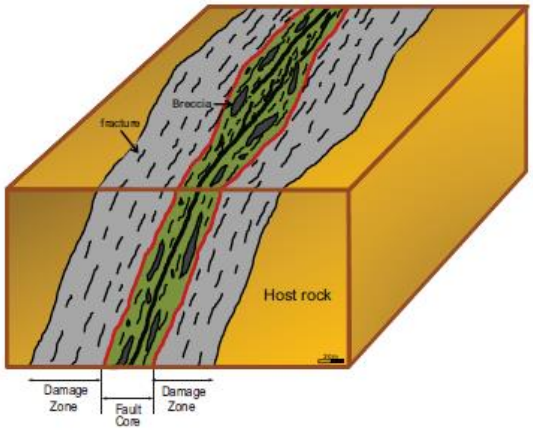

Figure 3.1 Typical fault zone structure with a single fault core surrounded by a fractured damage zone (Ligtenberg *et al.*, 2011).

3.1.1.1 Fluid flow properties of faults

Fluid flow properties of fault zones generally depend on several factors such as the host rock lithology, the amount of shale in the surrounding rocks, the dip and strike of faults, the fault throw, the tectonic history and fault diagenesis.

The juxtaposition pattern of different lithological units across a fault is of primary importance for prediction of fault sealing behaviour. The sealing behaviour can arise from a juxtaposition seal (i.e. reservoir-against-nonreservoir juxtaposition) or a fault rock seal (i.e. reservoir-against-reservoir juxtaposition). In the case of a juxtaposition seal, faults are acting as barriers to fluid flow. In the case of a fault rock seal, this is often not the case. Analysis of the petrophysical properties of fault rocks gathered from over 50 oil and gas fields in the North Sea and Norwegian Continental Shelf by Fisher and Knipe (2001) showed that in many cases faults are likely to allow some flow to occur. In this case, faults are partially transmissible and act as flow baffles.

The common way of modelling faults in industry-standard fluid flow simulators is to introduce transmissibility multipliers (e.g. Jolley *et al.*, 2007). Transmissibility multipliers are the derived numerical parameters assigned to grid-blocks or grid-block faces adjacent to faults in order to take into account the influence of fault rocks on fluid flow. Transmissibility multipliers are generally a function of the fault zone and of the grid-blocks to which they are assigned. In the method proposed by Manzocchi *et al.* (1999), the fault is conceptualized as a volume of a particular thickness and shale content, and the proportion of shale in the volume is assumed to be the main control on the fault permeability. The latter was also evident from experimental data, which showed that the permeability reduced log-linearly over four orders of magnitude with increasing clay content (Crawford *et al.*, 2008). The shale content of the fault zone is calculated as a function of the faulted sequence using the Shale Gouge Ratio (SGR) method. The SGR method is generally applicable to clastic (sand-shale) sequences. The SGR method calculates the proportion of shale along each part of the fault (Yielding *et al.*, 1997; Yielding, 2002). For a sequence of reservoir layers of different thickness and shale content, the SGR-value can be calculated using the following expression:

Copyright © MiReCOL Consortium 2014-2017

$$SGR = \frac{\sum (Vsh * \Delta z)}{t} x100\% \quad \text{(Eq. 3.1)}$$

SGR is the Shale Gouge Ratio, Vsh is the shale content in a particular layer, Δz is the thickness of a particular layer and t is the fault throw.

In the next step an empirical relation can be used to predict fault zone permeability as a function of shale content (calculated by the SGR method) and fault displacement. Finally, an up-scaled fault transmissibility value can be derived, which is equal to the mean permeability of the juxtaposed cells, weighted by the cross-sectional contact area and the inverse of the distance between their centers (for details refer to Manzocchi *et al.*, 1999).

Another method for calculation of transmissibility multipliers proposed by Zijlstra *et al.* (2007) can account for the two-phase flow properties of fault rocks. This is done by: (i) making the faults totally sealing to gas for a height above the free water level determined from the capillary entry pressure of the fault rock; and (ii) at greater distances above the free water level relative transmissibility multipliers are calculated based on estimates of the relative permeability of the fault rock. The authors present successful application of the method in three North Sea field simulation studies.

3.1.1.2 Geomechanical properties of faults

Fault zone mechanical properties and fault mechanics have been extensively studied in relation to earthquakes, which are the results of ruptures due to shear failure along pre-existing faults (Scholz, 2002).

Mechanical properties of fault zones, similar to fluid flow properties, depend on several factors such as the host rock lithology, fault-gouge composition, fault zone diagenetic history, offset, etc.

Elastic properties

The elastic properties of fault zones show a reduction in Young's modulus and an increase in Poisson's ratio with increasing damage within the damage zone to the fault core (Faulkner *et al.*, 2006).

Shear strength and constitutive models for shear failure

Shear failure of a fault can be brittle or ductile. Earthquakes result from brittle failure, which has been studied far more extensively in the literature than ductile failure. Brittle shear failure under compressive stress states is commonly described with the empirical Coulomb failure criterion:

$$\tau = c + \mu_s \sigma_n^{'} \quad \text{(Eq. 3.2)}$$

τ is the critical shear stress at failure, c is the cohesion and μ_s is the static friction coefficient which can be calculated as $\mu_s = \tan(\varphi)$ (φ is the friction angle).

The fluid pressure is coupled to the stress by the effective stress law of Terzaghi:

$$\sigma_n^{'} = \sigma_n - p \quad \text{(Eq. 3.3)}$$

Copyright © MiReCOL Consortium 2014-2017

σ_n' is the effective normal stress acting on a fault, σ_n is the total normal stress and p is the fluid pressure.

The coupling between the fluid pressure and the stress enables estimation of the fluid pressures required to initiate shear failure and fault reactivation in a CO_2 storage reservoir.

The static coefficient of friction varies between 0.6 and 0.85 (Byerlee, 1978). This range is valid for different mineralogical composition with exception of phyllosilicates and rock salts, where coefficients of friction are typically lower (e.g. Moore and Rymer, 2007). A frictional coefficient of 0.6 is, in many cases, adopted as a lower limit value, and faults are assumed cohesionless.

Coulomb failure criterion with the static coefficient of friction is, however, not sufficient to describe dynamic fault rupture. Experimental data showed that the force necessary to initiate the shear movement along two surfaces in contact is larger than the force required to maintain the motion. Therefore two coefficients of friction were distinguished: the static coefficient of friction (μ_s), which is necessary to initiate sliding, and the kinetic or dynamic coefficient of friction (μ_{ks}), which is necessary to maintain sliding.

Static friction was found to increase logarithmically with hold time. The kinetic coefficient of friction was observed to vary with sliding velocity; it may either become stronger (velocity strengthening) or weaker (velocity weakening).

Rabinowicz (1951) showed experimentally that the static and kinetic friction can be related. The transition from static to dynamic friction occurs over a critical distance D_c. This led to the development of a slip weakening law (Figure 3.2). An important shortcoming of this law is that it can not account for healing and is therefore limited to one stick-slip cycle.

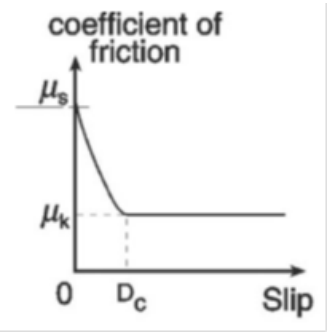

Figure 3.2 Linear slip weakening law showing the transition between static and dynamic friction during sliding (Rabinowicz, 1951).

The shortcoming of a slip weakening law was overcome by an empirical Rate-and-State Friction (RSF) model, which can describe many aspects of the observed seismic and inter-seismic frictional behavior (e.g. pre-seismic slip, earthquake nucleation, after-slip, etc.; Dieterich, 1979; Ruina, 1983; Marone, 1998). The RSF does not make a distinction between a static and dynamic friction coefficient; it uses a single coefficient of friction,

Copyright © MiReCOL Consortium 2014-2017

which is a function of sliding velocity and a state variable θ that represents a memory of past sliding history. The expressions to calculate the friction coefficient and the evolution of a state variable according to Dieterich (1979) are as follows:

$$\mu = \mu_0 + a\ln\left(\frac{V}{V_0}\right) + b\ln\left(\frac{V_0\theta}{D_c}\right), \qquad \frac{d\theta}{dt} = 1 - \left(\frac{V\theta}{D_c}\right) \qquad \text{(Eq. 3.4)}$$

μ_0 is the steady state friction coefficient at reference velocity V_0, V is the new velocity, D_c is the characteristic or critical slip distance (equal to the distance required for the frictional resistance to reach 1/e of its original value) and a and b are dimensionless empirical parameters. D_c, a and b are determined from laboratory data in which velocity is changed (Figure 3.3).

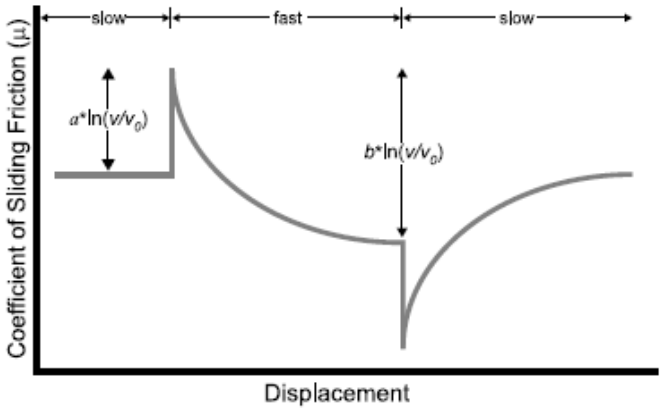

Figure 3.3 Results from velocity step experiments are shown to illustrate the concept of rate-and-state dependent friction. Idealized frictional response in velocity step experiments in which a gouge layer is sheared until a friction has reached a steady state and then the velocity is changed instantaneously. For a step increase in loading velocity, friction increases by a*ln(V/V0) and then decays over a characteristic sliding distance (Dc) by an amount b*ln(V/V0) to a new steady state value. (a-b)>0 implies a velocity strengthening material. (a-b)<0 (as in the figure) is a velocity weakening material (Samuelson et al., 2009).

Tensile strength and tensile failure

Tensile opening of a single fracture in Mode I will occur when the effective normal stress acting on a cohesionless fault becomes tensile. Possible cause for fracture dilation and opening is pore pressure increase within the fracture (Eq.3.5).

Hydromechanical behaviour of faults

Fault zone permeability predicted by a fault seal algorithm (such as the SGR method described earlier) can be changed on production/injection time-scales due to geomechanical effects. Production- or injection-related geomechanical stress changes, arising from pore pressure changes, can trigger fault slip and re-activate faults changing

Copyright © MiReCOL Consortium 2014-2017

(mainly increasing) their permeability. Coupling of the interactions between fluid flow and related geomechanical effects on faults cannot be done in production simulation models as they do not have appropriate constitutive models for frictional fault behavior, which are available in coupled stress-flow simulators.

Modelling of coupled deformation and permeability evolution during fault re-activation was performed in the context of geological CO_2 sequestration to assess the geological risks of induced seismicity and fluid leakages (Rutqvist *et al.*, 2007). Cappa and Rutqvist (2011) describe three modeling approaches that have been considered to analyze multi-phase fluid flow and stress coupling with the TOUGH-FLAC simulator. Fault behavior was represented in hydromechanical models using slip zero-thickness interface and finite-thickness elements with isotropic or anisotropic elasto-plastic constitutive models. The results of this investigation showed that fault hydromechanical behavior can be appropriately represented with the least complex alternative, using a finite-thickness element and isotropic plasticity.

In the context of petroleum production, fault behavior is incorporated in coupled hydromechanical models developed to assess the potential for fault re-activation either as a cause of seismicity or well damage, and rarely in connection to fluid migration. An example of the latter is given in Cuisat *et al.* (2010). The study objective was to assess the potential for developing hydraulic communication between Statfjord and Snorre fields separated by a horst structure during final depressurization of the Statfjord field. Mechanical and sealing integrity of the horst-bounding faults and the horst structure were assessed by coupled single-phase fluid flow and elastic stress simulations with the Plaxis simulator. The results indicated that the geomechanical stress changes and the associated deformation will not affect significantly sealing integrity of faults.

The initial stress field (i.e. pre-depletion for CO_2 storage in depleted gas fields) can significantly affect fault zone permeability. According the critically-stressed-fault hypothesis by Zoback (2007, p.341), faults, which are in a state of failure equilibrium, are hydraulically conductive. This is supported by deep crustal permeability data acquired from *in situ* hydraulic tests and induced seismicity (Townend and Zoback, 2000). Critically stressed faults with a static friction coefficient μ=0.6 to 1.0 have *in situ* permeability in the range 0.01 to 0.1 mD, which is three to four orders of magnitude higher than measured on core samples. However, the hypothesis of the critically stressed deep subsurface is not generally applicable to shallower depths (< 4 km) where depleted gas reservoirs, which could be used for CO_2 storage, are usually found. For example, the faults involved in induced seismicity associated with gas extraction in the Netherlands are not critically stressed at the onset of depletion. This can explain the delay of seismic events which occur not prior to 28% of depletion (Van Wees *et al.*, 2014).

3.1.2 Hydraulic fracturing

Hydraulic fracturing is a well stimulation technique to increase the productivity of hydrocarbon production wells. Wells are stimulated by initiating and propagating a tensile fracture from wellbore into the hydrocarbon-bearing rock formation by injecting large quantities of fluids at high pressure. Hydraulic fractures, varying in length from a few meters to a few hundreds of meters, are formed perpendicular to the minimum in

Copyright © MiReCOL Consortium 2014-2017

situ stress direction. The technique has been in use in the oil and gas industry since 1947 (DOE, 2004).

Hydraulic fracturing is used in both conventional and unconventional reservoirs. In conventional reservoirs, fracturing is typically used to: (i) increase the permeability of reservoirs; (ii) restore the impaired permeability in the near well area; and (iii) control sand production. Besides improving well production, conventional reservoirs are fractured to increase the injectivity of rock formation for re-injection of produced water (PWRI) or slurry containing drill cuttings. In unconventional reservoirs, hydraulic fracturing is used for stimulations of shale formations, coalbed methane reservoirs and geothermal systems. In the mining industry, hydraulic fracturing is sometimes used for pre-conditioning of the rock to promote caving during mining operations.

Small scale fracturing is used in field tests to measure the in situ stresses and to aid the design of conventional fracturing treatments. In these tests a very small hydraulic fracture (a few decimeters to a few meters) is induced by pumping a small quantity of the injected fluid, compared to the conventional fracturing, without proppant. The field tests comprise micro- and a mini-frac tests, leakoff and extended leakoff tests, etc..

In conventional reservoirs, hydraulic fracturing commonly creates a single fracture that propagates in two directions from the wellbore forming two wings (Figure 3.4). The commonly used geometry models for a fracture comprise a vertical (or horizontal) ellipsoidal fracture (Figure 3.4a) or a constant height fracture (Figure 3.4b). The geometry of the created fracture is primarily driven by the *in situ* stress field with fracture growth perpendicular to the direction of the least principal stress. Other reservoir parameters controlling the fracture growth include the layering or interfaces between different rock strata and the mechanical properties of these strata. In addition, the fracture growth will be affected by the fracture treatment itself, the characteristics of the fraccing fluid, chemical reactions between the fluid and the rock, etc..

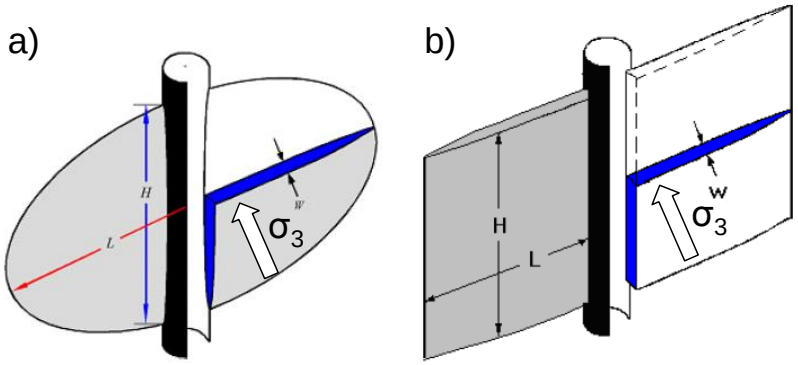

Figure 3.4 a) Vertical ellipsoidal fracture geometry and b) constant height fracture geometry (Meyer, 2013). The fracture is induced at 90° to the direction of the minimum in situ stress σ_3.

In unconventional reservoirs and naturally fractured reservoirs, hydraulic fracturing induces fractures that propagate and interact with a system of natural fractures already present in the reservoir rock. The interaction between an induced fracture and a natural fracture system, i.e. a Discrete Fracture Network (DFN), is usually quite complex (as illustrated in Figure 3.5). The most recent advances in fracturing of unconventional

Copyright © MiReCOL Consortium 2014-2017

reservoirs have been achieved in development of shale gas resources. In shale gas development, aggressive hydraulic fracturing is used to generate an interconnected open fracture network with a large internal surface area for gas drainage towards a well. The emplacement of horizontal wells more than 1 km long, which became economical by the late 1990's, and development of Multi-Stage Hydraulic Fracturing[1] (MSHF) in the period 2000–2008, are the two key technologies that made the "shale gas revolution" in the United States and Canada possible (Dusseault, 2013).

Horizontal drilling and MSHF are the two technologies particularly relevant for the CO_2 mitigation scenario described in section 3.1.3 in which the MSHF from a long horizontal well will be used to connect two neighboring reservoir compartments.

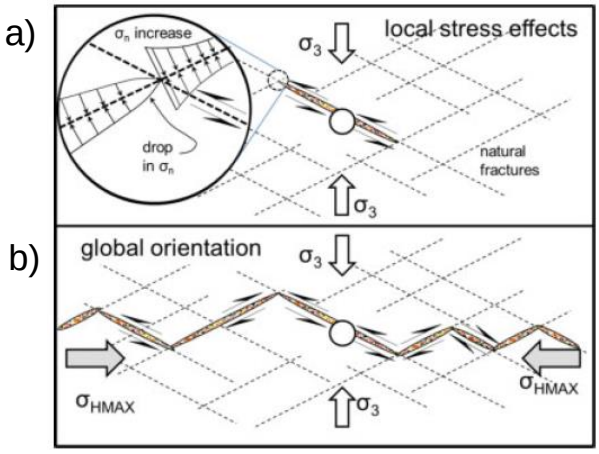

Figure 3.5 a) Local and b) large scale effects on fracture propagation in naturally fractured formation (Dusseault, 2013). At the local scale, a fracture will tend to follow approximately natural fractures rather than initiate new ones through the intact rock. At the large scale, the fractures will tend to remain on average at 90° to the direction of σ3.

3.1.2.1 Hydraulic fracturing across geological discontinuities

The flow diversion option of transferring CO_2 to a neighboring compartment by a fault-seal breach requires consideration of the interaction between a hydraulic fracture propagating from the wellbore and an existing fault. A brief literature review showed that this particular topic has been explored in only a limited manner, typically considering the interaction between two discrete mechanical discontinuities representing a hydraulic fracture and a natural fracture. Representing a fault with a single discontinuity may not always be sufficient because the fault architecture is usually more complex: it comprises the damaged rock, the fault gouge and several slip surfaces, with the distinct material properties. The literature on hydraulic fracturing mainly focuses on the fracture design and prediction of fracture initiation and growth.

[1] Creation of hydraulic fractures at multiple locations in a single well.

Copyright © MiReCOL Consortium 2014-2017

The criterion for fracture initiation was defined by Haimson and Fairhurst (1967): a fracture will be initiated when the fluid pressure in the wellbore exceeds the minimum in situ stress (assuming that the host rock has a negligible tensile strength).

Early studies carried out in 1980's focused on determining the factors affecting the propagation and containment of a hydraulic fracture in a layered rock mass. Anderson (1979) conducted hydraulic fracture experiments to observe the growth of hydraulic driven fractures in the vicinity of an unbonded interface in rocks. The two factors were identified which determine whether a hydraulic fracture would cross the interface: the normal stress acting on the interface and the frictional properties of the interface.

Teufel and Clark (1984) demonstrated that two distinct geologic conditions can inhibit or contain the vertical growth of hydraulic fractures in layered rock: a weak interfacial shear strength of the layers and an increase in the minimum horizontal *in situ* stress in the bounding layers. The *in situ* stress distribution is thought to be more important for the fracture growth and containment. Differences in elastic properties within a layered rock mass could also be important because variations in elastic properties influence the vertical distribution of the minimum horizontal stress.

The importance of the *in situ* stress distribution on fracture growth was also observed in the field tests and the mineback experiments carried out by Warpinski and Teufel (1987; Figure 3.6). The confinement resulting from a high-stress region is a first order effect, whereas interfaces, strength changes, fluid pressure gradients have only second-order effects on fracture growth. Geologic discontinuities can affect the overall geometry of hydraulic fractures by arresting the growth of the fracture, increasing fluid leakoff, enhancing the creation of multiple fractures, etc.. The ability of a crack to propagate across the natural discontinuity depends on the in-situ stresses and the coefficient of friction of the interface. Fractures will generally cross discontinuities at high angles of approach and large stress differences (Figure 3.6).

Zhang and Jeffry (2004) developed a numerical fracture model for solving the problem of coupled rock deformation, fluid transport and interface slip associated with hydraulic fracture propagation across frictional interfaces. The authors found that the approaching hydraulic fracture can induce a new fracture in rocks of low tensile strength. However, there is a critical range of tensile strengths that result in the fracture penetrating the interface without offset. Beyond the maximum of this range, the fracture cannot induce a new fracture, based on the tensile strength criterion and is diverted into and grows along the interface instead.

Wu *et al.* (2004) demonstrated both numerically and experimentally that when a fracture propagates from a rigid layer toward a softer layer, the fracture will break through the interface. However, when a fracture propagates from a soft layer to a rigid or stiffer layer, crack arrest can occur and other fracture mechanisms such as the formation of secondary fractures across the interface (again leading to fracture breakthrough), delamination along the interface, or crack kinking resulting in fracture containment, can occur. The authors proposed a fracture mechanisms map (FMM) in the vicinity of an interface to assist in hydraulic fracture treatment design.

Copyright © MiReCOL Consortium 2014-2017

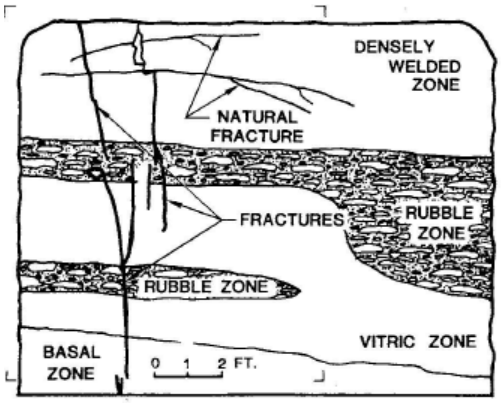

Figure 3.6 Complex fracture behavior from a mineback experiment at the Nevada Test Site in the U.S. The sketch shows that induced fractures intersect the natural fracture system (Warpinsky and Teufel, 1987).

Chuprakov *et al.* (2013) studied hydraulic fracture propagation across a weak discontinuity controlled by fluid injection. This research was mainly focused on the result of fracture interaction in terms of crossing or arresting of the hydraulic fracture at the natural fracture. The key parameters controlling the crossing/non-crossing interaction behavior were identified: in-situ stress parameters, interaction angle, the injection rate, viscosity of fracturing fluid and the fracture aperture. When the pre-existing aperture of the natural fracture is as large as that of the hydraulic fracture, the hydraulic fracture is likely to arrest.

One case was reported of hydraulic fracturing during a gas well stimulation, which induced movement on a nearby fault (Maxwell *et al.*, 2009).

3.1.2.2 Implications for fracture containment in CO_2 storage reservoirs

Practical implications of the importance of stress distribution on fracture containment are that it is much easier to constrain the vertical fracture growth in a depleted gas reservoir (being re-filled with CO_2) than in an aquifer. In the case of CO_2 storage in a depleted gas reservoir, the minimum in situ stress in the reservoir will be lower than in the pre-depleted state (assuming a normal-faulting stress regime and re-pressurization with the injected CO_2 below the initial reservoir pressure) while the stress in the caprock will stay largely unchanged. Change in the minimum in situ stress in the reservoir due to pore pressure change can be estimated by the following expression:

$$\Delta Sh\min = \alpha\, dP \frac{1-2\nu}{1-\nu} \qquad \text{(Eq. 3.5)}$$

$\Delta Sh\min$ is the minimum stress change, α is the Biot's constant, dP is the depletion and ν is the Poisson's ratio.

The minimum stress in the caprock will always be higher than the pressure in a depleted, or partially re-pressurized, storage reservoir. As a consequence, the vertical growth of a hydraulic fracture will be naturally constrained by the presence of a high-

Copyright © MiReCOL Consortium 2014-2017

stress region in the caprock. In contrast to the CO_2 storage in a depleted reservoir, the minimum in situ stress in the reservoir will be increasing during the CO_2 injection, and the vertical fracture growth will be difficult to constrain.

3.1.2.3 Hydraulic fracturing simulators

Fracture design and treatment rely on a good understanding and prediction of fracture initiation and growth. Hydraulic fracturing simulators are used for the design, analysis and monitoring of hydraulic fractures (Figure 3.7 and Figure 3.8). The first simulators appeared in the late 1980's (Meyer, 1989). Nowadays, fracturing simulators are developed and used as in-house tools in some of the major oil companies (e.g. Van den Hoek *et al.*, 1999; Noirot *et al.*, 2003) or are available as commercial software packages (e.g. the Meyer Fracturing Software suite; Meyer, 2013). The Meyer fracturing simulator, which is a state-of-the-art fracturing simulator with several modules. The most relevant modules are those for simulating fracture propagation as well as the interaction between the hydraulic fracture and natural fractures or a fault. These modules are:

- MFrac - a three-dimensional hydraulic fracturing simulator accounting for the coupled parameters affecting fracture propagation and proppant transport, and including three-dimensional fracture geometry.
- MPwri – a three-dimensional hydraulic fracturing waterflood simulator designated for simulating produced water reinjection (PWRI).
- MShale - a Discrete Fracture Network (DFN) simulator designated for simulating three-dimensional hydraulic fracture propagation in discrete fracture networks.

The major fracture, rock and fluid mechanics phenomena included in the Meyer suite of fracturing simulators are: (1) multilayer unsymmetrical confining stress contrast; (2) multilayer leakoff; (3) fracture toughness and dilatancy (tip effects); (4) variable injection rate and time dependent fluid rheology; (5) vertical and lateral rock deformation; (6) wall roughness and (7) coupled proppant transport, heat transfer and fracture propagation (Appendix A; Meyer, 2013).

The shortcomings of the MFrac/MShale are due to the following assumptions: (1) horizontal layering; (2) homogeneity in the rock properties within model layer; (iii) pre-defined and simple geometry of the DFN represented by two orthogonal fracture systems; (iv) simple criteria for fracture initiation and propagation.

Copyright © MiReCOL Consortium 2014-2017

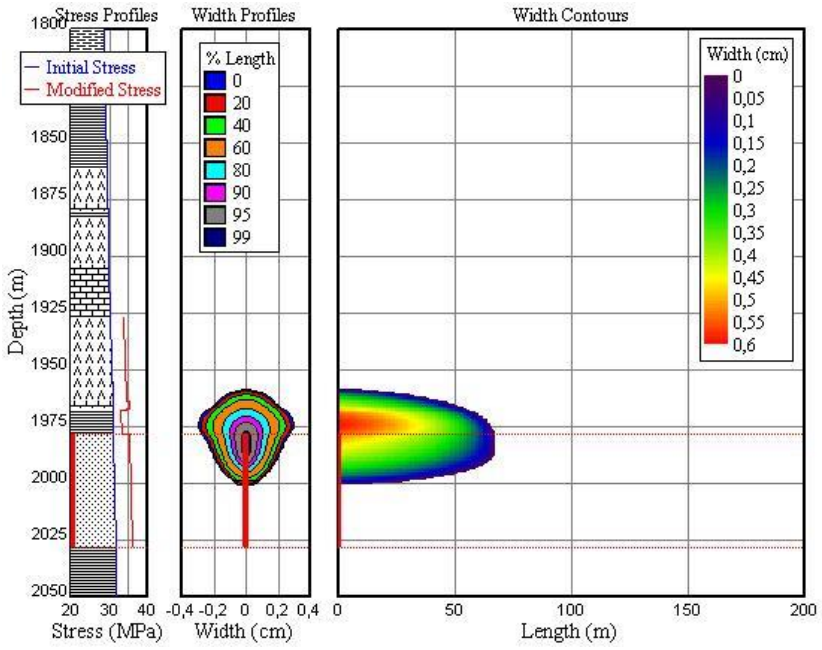

Figure 3.7 Typical simulation of hydraulic fracture obtained using MFrac/MPwri fracturing simulator. The graphs show (from left to right) stress profiles, width profiles and contours of the hydraulic fracture (Hofstee *et al.*, 2009).

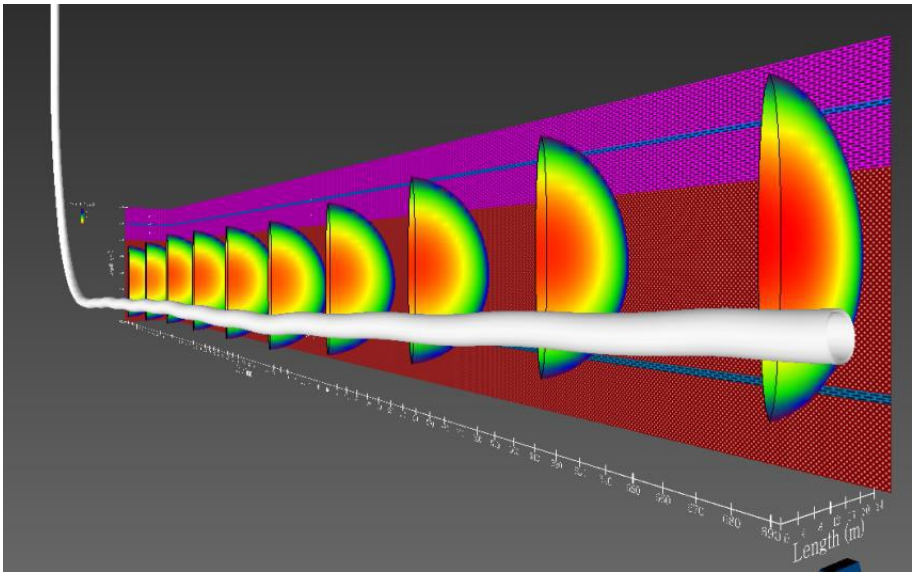

Figure 3.8 Simulation of multistage hydraulic fracturing from a horizontal well using MFrac/MShale (source: TNO).

3.1.3 Model requirements and description of the CO_2 mitigation scenarios

The CO_2 mitigation scenario considers flow diversion to a neighbouring compartment separated by a fault from the main compartment, which shows signs of leakage of

Copyright © MiReCOL Consortium 2014-2017

deviations from the expected flow behaviour. The fault seal has to be breached in order to make transferring of CO_2 between the compartments possible. Seal breach can be attempted by multistage hydraulic fracturing from a horizontal well drilled through the main compartment approximately parallel to the fault strike.

Model requirements

The reservoir model should represent a compartmentalized gas field or aquifer initially without cross fault communication between neighbouring compartments. The main reservoir and the neighbouring compartment planned to be used for flow diversion must be partially juxtaposed. Fluid pressure in the neighbouring compartment should preferably be lower than in the main compartment to facilitate buoyancy-driven CO_2 flow during flow diversion. The latter requirement is fulfilled when the neighbouring compartment is upthrown and/or depleted. The model must contain migration pathways for CO_2 leakage through the fractured caprock or reservoir bounding faults.

Description of the model selected

A geological setting suitable to investigate the feasibility of remediation by flow diversion comprises a compartmentalized gas reservoir or aquifer. Such structural settings are quite common: e.g. the depleted P18-4 gas reservoir, planned to be used for CO_2 storage in the Rotterdam Capture and Storage Demonstration Project (ROAD), is separated by a sealing fault from the neighbouring P15 depleted gas field (Figure 3.9). The feasibility of CO_2 storage in the depleted P18-4 gas reservoir was studied in the Dutch national programme on Carbon Capture and Storage - CATO-2 (Arts *et al.*, 2012, Arts *et al.*, 2011; Vandeweijer *et al.*, 2011).

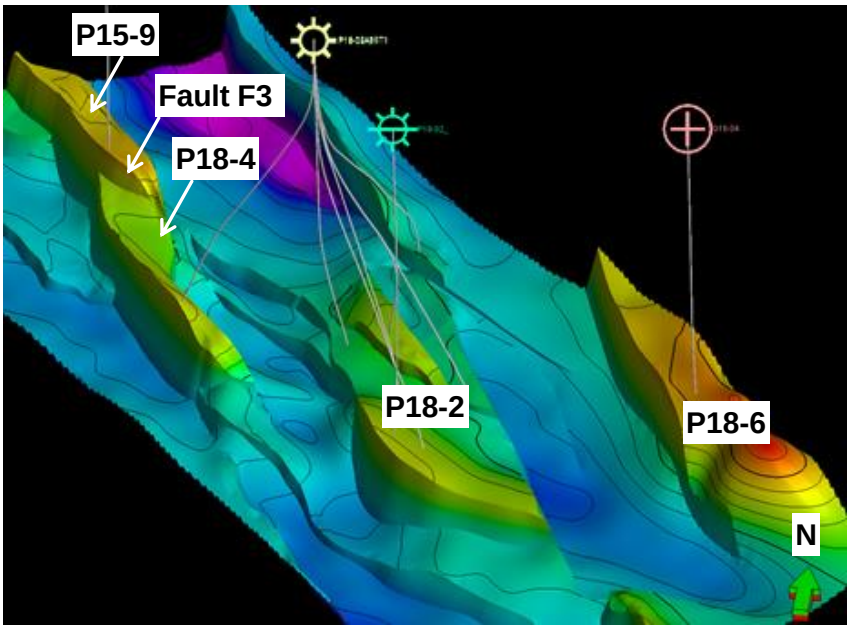

Figure 3.9 An example of the structural setting with two neighboring depleted gas reservoirs separated by a sealing fault (P18-4 and P15; Arts *et al.*, 2012).

Copyright © MiReCOL Consortium 2014-2017

Another field example relevant for CO_2 storage in both depleted gas fields and aquifers, are the Rotliegendes reservoir rocks, which are compartmentalized in the Netherlands and also throughout north-western Europe (Figure 3.10).

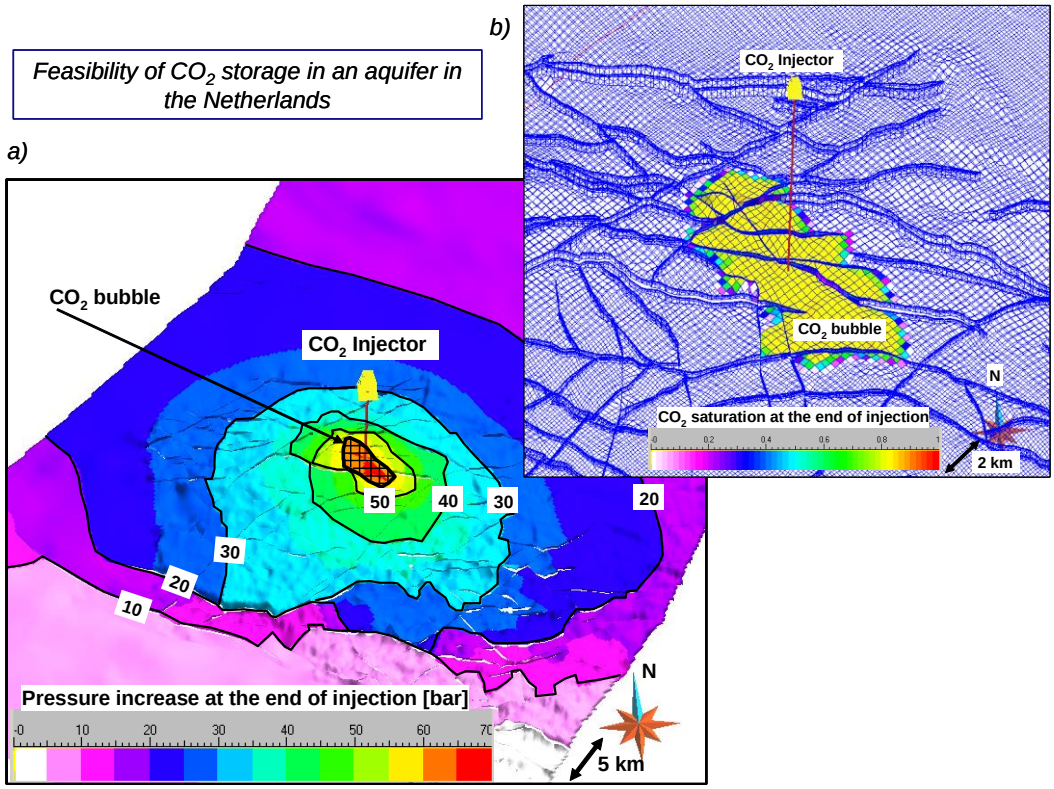

Figure 3.10 An example of the structural setting with multiple aquifer compartments. Reservoir simulation results of CO_2 injection assuming that all the faults are conductive. a) Footprint area of elevated pressures; b) footprint area of the CO_2 plume (Orlic *et al.*, 2011).

Planned model procedure

The feasibility of remediation by flow diversion will be tested in a follow-up study on a generic model with two reservoir compartments separated by a sealing fault (Figure 3.11). Leakage scenarios may consider leakage through one of the bounding faults, implemented as a line sink, and leakage through the caprock, implemented as an areal sink. The geometry of the compartments in the synthetic model will be fairly simple. Models with various fault offsets can be considered (e.g. 10 to 50%). Also, differences in permeability between the two neighbouring compartments can be considered, e.g. the case where a low-permeability reservoir is juxtaposed against a high-permeability reservoir, and vice-versa. Various grid configurations and resolutions can be explored for inclusion of hydraulic fractures in a reservoir simulation grid. The initial volumes of gas, the volumes of gas produced and CO_2 injected in a generic model will be kept realistic for the case of industrial-scale CO_2 storage. The effects of flow diversion as a

Copyright © MiReCOL Consortium 2014-2017

mitigation measure can be tested for the option of CO_2 storage in a depleted gas field and in an aquifer.

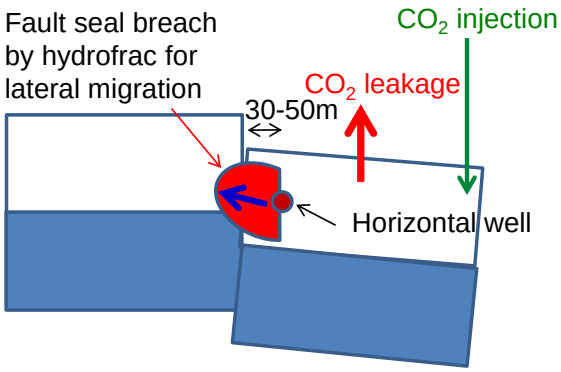

Figure 3.11 Side-view of a generic model with two reservoir compartments separated by a sealing fault. Connection to a neighbouring compartment for diversion of CO_2 is achieved by hydraulic fracturing.

In the second phase of the project, a realistic field-scale model with two neighbouring compartments will be developed. Model adjustments can be implemented based on the outcome of generic model simulations. Envisaged leakage scenarios are the same for the generic and the realistic model: a leakage through a bounding fault and a leakage through the caprock. The leakage may be initiated at the start of injection period or at some point during injection. The total amount of CO_2 that escaped from the storage reservoir must be above detectable thresholds before starting the proposed mitigation action: drilling a new well and creating hydraulic fractures through the fault seal to connect with the nearby compartment. Geometry and hydraulic properties of induced fractures will be obtained from hydraulic fracturing simulations. Transmissibility multipliers will be derived from fracturing simulations and applied in a realistic reservoir simulation model to account for the fluid flow through the newly created hydraulic fractures.

Simulations will be used to investigate:

- The diversion rates through a single and multiple hydraulic fractures.
- The effect of fracture dimensions and flow properties on the diversion rates.
- The duration needed to release the reservoir pressure and the leakage rates to an admissible level.

3.1.4 Concluding remarks

A CO_2 mitigation scenario by flow diversion from the main, leaky compartment to a neighbouring compartment separated by a sealing fault, has been developed. The fault seal must be breached in order to make transferring of CO_2 between two neighbouring compartments possible. Seal breach can be attempted by multistage hydraulic fracturing from a new horizontal well drilled approximately parallel to the fault strike. Several newly created hydraulic fractures will act as high-permeability pathways for CO_2 migration from the main reservoir to a neighbouring compartment in the storage

Copyright © MiReCOL Consortium 2014-2017

reservoir, releasing the pressure and decreasing the migration rates out of the main reservoir.

The feasibility of the described CO_2 mitigation scenarios will be investigated by numerical simulations of fluid flow in a fault-compartmentalized gas reservoir or aquifer. The CO_2 mitigation scenario by flow diversion will be first tested on a generic model, which consists of two reservoir compartments, separated by a sealing fault. The role of key parameters controlling CO_2 migration between two compartments, such as the number and the flow characteristics of hydraulic fractures, will be investigated. In the subsequent phase a realistic reservoir model will be used.

4 REFERENCES

1. Alassi, H.T., Holt, R., Nes, O.-M., Pradhan, S., 2011. Realistic geomechanical modeling of hydraulic fracturing in fractured reservoir rock. CSUG/SPE paper 149375, in the *Canadian Unconventional Resources Conference* held in Calgary, Alberta, Canada, 15-17 November 2011.
2. Anderson, G.A., 1979. Effects of friction on hydraulic fracture growth near unbonded interfaces in rock, *SPE 54th Annual Technical Conference and Exhibition*, Las Vegas, SPE 8347.
3. Arts, R., Hofstee, C., Vandeweijer, V., Pluymaekers, V., Loeve, D., Orlic, B., Koenen, M., Tambach, T., Spiers, C., Samuelson, J., 2011. *Status report on remaining issues identified after the feasibility study for CO_2 injection in the depleted P18 gas field.* CATO-2 report CATO-2-WP3.9-D14.
4. Arts, R.J, Vandeweijer, V.P, Hofstee, C., Pluymaekers, M.P.D., Loeve, D., Kopp, A., Plug, W.J., 2012. The feasibility of CO_2 storage in the depleted P18-4 gas field offshore the Netherlands (the ROAD project), *International Journal of Greenhouse Gas Control, 11*, S10–S20.
5. Bahat, D., Rabinovitch, A., Frid, V., 2005. *Tensile Fracturing in Rocks: Tectonofractographic and Electromagnetic Radiation Methods*, 584, Springer, Berlin.
6. Brown, S.R., 1987. Fluid flow through rock joints: the effect of surface roughness, *Journal of Geophysical Research*, B, 92, 1337-1347.
7. Byerlee, J.D., 1978. Friction of rocks, *Pure and Applied Geophysics*, 116: 615-626.
8. Cappa, F., Rutqvist, J., 2011. Modeling of coupled deformation and permeability evolution during fault reactivation induced by deep underground injection of CO_2, *International Journal of Greenhouse Gas Control*, 5, 336–346.
9. Chuprakov, D., Melchaeva, O., Prioul, R., 2013. Hydraulic fracture propagation across a weak discontinuity controlled by fluid injection, In Bunger, McLennan, and Jeffrey (eds): *Proceedings of the International Conference for Effective and Sustainable Hydraulic Fracturing*, An ISRM specialized Conference, Brisbane, Australia, May 2013, http://dx.doi.org/10.5772/55941.
10. Crawford, B.R., Faulkner, D.R., Rutter, E.H., 2008. Strength, porosity, and permeability development during hydrostatic and shear loading of synthetic quartz-clay fault gauge, *Journal of Geophysical Research*, 113, B03207, doi:10.1029/2006JB004634.

Copyright © MiReCOL Consortium 2014-2017

11. Cuisat, F., Jostad, H.P., Andresen, L., Skurtveit, E., Skomedal, E., Hettema, M., Lyslo, K., 2010. Geomechanical integrity of dealing faults during depressurisation of the Statfjord Field, *Journal of Structural Geology*, 32, 1754-1767.
12. Cuss, R. J., Milodowski, A., Harrington, J. F., 2011. Fracture transmissivity as a function of normal and shear stress: First results in Opalinus Clay, *Physics and Chemistry of the Earth, Parts A/B/C*, 36, 1960-1971.
13. DOE, 2004, Department of Energy - *Hydraulic Fracturing White Paper*, Appendix A, EPA 816-R-04-003.
14. Dieterich, J. H., 1979. Modeling of rock friction 1. Experimental results and constitutive equations, *Journal of Geophysical Research B: Solid Earth*, 84(B5), 2161-2168.
15. Dusseault, M., 2013. Geomechanical aspects of shale gas development, In *Proceedings of EUROCK 2013 - The 2013 ISRM International Symposium*, M. Kwaśniewski and D. Łydżba (eds.), Wrocław, 21-26 September, 969-975, London, Taylor & Francis Group.
16. Edlmann, K., Haszeldine, S., McDermott, C.I., 2013. Experimental investigation into the sealing capability of naturally fractured shale caprocks to supercritical carbon dioxide flow, *Environmental Earth Science*, 70(7), 3393-3409.
17. Esaki, T., Du, S., Mitani, Y., Ikusada, K., Jing, L., 1999. Development of a shear-flow test apparatus and determination of coupled properties for a single rock joint, *International Journal of Rock Mechanics and Mining Sciences*, 36(5), 641-650.
18. Faulkner, D.R., Jackson, C.A.L., Lunn, R.J., Schlisch, R.W., Shipton, Z.K., Wibberley, C.A.J., Withjack, M.O., 2010. A review of recent developments concerning the structure, mechanics and fluid flow properties of fault zones, *Journal of Structural Geology*, 32, 1557-1575.
19. Faulkner, D.R., Mitchell, T.M., Healy, D., Heap, M.J., 2006. Slip on 'weak' faults by the rotation of regional stress in the fracture damage zone, *Nature*, Letters, 444, 922-925.
20. Fessenden, J.E., Stauffer, P.H., Viswanathan, H.S., 2009. *Natural Analogs of Geologic CO_2 Sequestration: Some General Implications for Engineered Sequestration*, in Geophysical Monograph Series. Vol.183, AGU.
21. Fisher, Q.J., Knipe, R.J., 2001. The permeability of faults within siliciclastic petroleum reservoirs of the North Sea and Norwegian Continental Shelf, *Marine and Petroleum Geology*, 18, 1063-1081.
22. Fjær, E., Holt, R.M., Horsrud, P., Raaen, A.M., Risnes, R., 2008. *Petroleum Related Rock Mechanics*, 2nd ed., 491, Elsevier, Amsterdam.
23. Friedman, S.J., 2007. Geological carbon dioxide sequestration, *Elements*, 3(June), 179-184.
24. Haimson, B.C., Fairhurst, C., 1967. Initiation and extension of hydraulic fractures in tocks, *Society of Petroleum Engineers Journal*, 7, 310-318, SPE 1710.
25. Hofstee, C., Benedictus, T., Ter Heege, J. H., Huibregtse, J., Van der Meer, B., Nelskamp, S., Orlic, B., Pluymaekers, M., Tambach, T., 2009. *Feasibility of CO_2 storage in the Friesland platform*, TNO Built Environment and Geosciences report TNO-034-UT-2009001084.
26. Jolley, S.J., Dijk, H., Lamens, J.H., Fisher, Q,J., Manzocchi, T., Eikmans, H., Huang, Y., 2007. Faulting and fault sealing in production simulation models: Brent Province, northern North Sea, *Petroleum Geoscience*, 13, 321-340.

Copyright © MiReCOL Consortium 2014-2017

27. Lakatos, I., Medic, B., Jovicic, D., Basic, I., Lakatos-Szabo, J., 2009. Prevention of vertical gas flow in a collapsed well using silicate/plolymer/urea method, *SPE International Symposium on Oilfield Chemistry*, Woodlands, Texas, SPE 121045.
28. Lavrov, A., 2013a. Numerical modeling of steady-state flow of a non-Newtonian power-law fluid in a rough-walled fracture, *Computers and Geotechnics*, 50(0), 101-109.
29. Lavrov, A., 2013b. Redirection and channelization of power-law fluid flow in a rough-walled fracture, *Chemical Engineering Science*, 99(0), 81-88.
30. Lavrov, A., Larsen, I., Holt, R.M., Bauer, A., Pradhan, S., 2014. Hybrid FEM/DEM simulation of hydraulic fracturing in naturally-fractured reservoirs. ARMA paper 14-7107, in the *48th US Rock Mechanics/Geomechanics Symposium* held in Minneapolis, MN, USA, 1-4 June 2014.
31. Lewicki, J., Birkholzer, J., Tsang, C.-F., 2007. Natural and industrial analogues for leakage of CO_2 from storage reservoirs: identification of features, events, and processes and lessons learned, *Environmental Geology*, 52(3), 457-467.
32. Ligtenberg, H., Okkerman, J., De Keijzer, M., 2011. Fractures in the Dutch Rotliegend – an overview, *Society for Sedimentary Geology Special Publication* 98, 229-244.
33. Magri, F., Tillner, E., Wang, W., Watanabe, N., Zimmermann, G., Kempka, T., 2013. 3D Hydro-mechanical Scenario Analysis to Evaluate Changes of the Recent Stress Field as a Result of Geological CO_2 Storage, *Energy Procedia*, 40(0), 375-383.
34. Manzocchi, T., Walsh, J.J., Nell, P.,Yielding, G., 1999. Fault transmissibility multipliers for flow simulation models, *Petroleum Geoscience*, 5, 53-63.
35. Marone, C., 1998. Laboratory-derived friction laws and their application to seismic faulting. *Annual Review of Earth and Planetary Sciences*, 26, 643-696.
36. Maxwell, S.C., Jones, M., Parker, R., Miong, S., Leaney, S., Dorval, D., D'Amico, D., Logel, J., Anderson, E., Hammermaster, K., 2009. Fault activation during hydraulic fracturing, *SEG Houston 2009 International Exposition and Annual Meeting*.
37. Meyer, B.R., 1989. Three-dimensional hydraulic fracturing simulation on personal computers: theory and comparison studies, *Eastern Regional SPE Meeting*, Morgantown, West Virginia, SPE 19329.
38. Meyer, B. R., 2013. *Meyer Fracturing Simulators, Programs and User's Guide* Tenth Edition, Baker Hughes Incorporated, Meyer Fracturing Software Group http://www.mfrac.com/.
39. Metz, B., Davidson, O., de Coninck, H., Loos, M., Meyer, L., 2005. *IPCC Special Report on Carbon Dioxide Capture and Storage*, Cambridge University Press, Cambridge.
40. Moore, E.D., Rymer, M.J., 2007. Talc-bearing serpentinite and the creeping section of the San Andreas fault. *Nature* 448:795–797.
41. Nelson, E.J., Hillis, R.R., Meyer, J.J., Mildren, S.D., Van Nispen, D., Briner, A., 2005. The reservoir stress path and its implications for water-flooding, Champion Southeast field, Brunei. ARMA/USRMS paper 05-775, in Alaska Rocks 2005, *The 40th U.S. Symposium on Rock Mechanics (USRMS): Rock Mechanics for Energy, Mineral and Infrastructure Development in the Northern Regions*, held in Anchorage, Alaska, June 25-29, 2005.

Copyright © MiReCOL Consortium 2014-2017

42. Nemoto, K., Moriya, H., Niitsuma, H., Tsuchiya, N., 2008. Mechanical and hydraulic coupling of injection-induced slip along pre-existing fractures, *Geothermics*, 37(2), 157-172.
43. Noirot, J.C., Van den Hoek, P.J., Zwarts, D., Bjoerndal, H.P., Stewart, G., Drenth, R., Al-Masfry, R., Wassing, B., Saeby, J., Al-Masroori, M., Zarafi., A., 2003. Water injection and water flooding under fracturing conditions, SPE 81462.
44. Oh, J., Kim, K.-Y., Han, W.S., Kim, T., Kim, J.-C., Park, E., 2013. Experimental and numerical study on supercritical CO_2/brine transport in a fractured rock: Implications of mass transfer, capillary pressure and storage capacity, *Advances in Water Resources*, 62, Part C(0), 442-453.
45. Orlic, B., ter Heege, J., Wassing, B., 2011. Assessing the integrity of fault- and top seals at CO_2 storage sites, *Energy Procedia*, 4(0), 4798-4805.
46. Pruess, K., Oldenburg, C., Moridis, G., 2012. *TOUGH2 User's Guide v2*..
47. Pyrak-Nolte, L. J., 1996. The seismic response of fractures and the interrelations among fracture properties, *International Journal of Rock Mechanics and Mining Sciences & Geomechanics Abstracts*, 33(8), 787-802.
48. Rabinowicz, E., 1951. The nature of the static and kinematic coefficients of friction, *Journal of Applied Physics*, 22, 1373-1379.
49. Raaen, A.M., Horsrud, P., Kjørholt, H., Økland, D., 2006. Improved routine estimation of the minimum horizontal stress component from extended leak-off tests, *International Journal of Rock Mechanics and Mining Sciences*, 43(1), 37-48.
50. Ruina, A., 1983. Slip instability and state variable friction laws, *Journal of Geophysical Research*, 88(B12), 10359-10370.
51. Rutqvist, J., Birkholzer, J.T., Cappa, F., Tsang, C.-F., 2007. Estimating maximum sustainable injection pressure during geological sequestration of CO_2 using coupled fluid flow and geomechanical fault-slip analysis, *Energy Conversion and Management*, 47, 1798–1807.
52. Samuelson, J, Elsworth, D., Marone, C., 2009. Shear-induced dilatancy of fluid-saturated faults: Experiment and theory, *Journal of Geophysical Research*, 114:B12404, doi:10.1029/2008JB006273.
53. Santarelli, F.J., Tronvoll, J.T., Svennekjaer, M., Skeie, H., Henriksen, R., Bratli, R.K., 1998. Reservoir stress path: the depletion and the rebound. SPE/ISRM paper 47350, in the SPE/ISRM Eurock'98 held in Trondheim, Norway, 8-10 July 1998.
54. Scholz, C.H., 2002. *The Mechanics of Earthquakes and Faulting* (second edition), Cambridge University Press.
55. Segall, P., Fitzgerald, S.D., 1998. A note on induced stress changes in hydrocarbon and geothermal reservoirs, *Tectonophysics*, 289(1–3), 117-128.
56. Sibson, R.H., 1996. Structural permeability of fluid-driven fault-fracture meshes, *Journal of Structural Geology*, 18(8), 1031-1042.
57. Streit, J.E., Hillis, R.R., 2004. Estimating fault stability and sustainable fluid pressures for underground storage of CO_2 in porous rock, *Energy*, 29(9–10), 1445-1456.
58. Teufel, L.W., Clark, J.A., 1984. Hydraulic fracture propagation in layered rock: experimental studies of fracture containment, *Society of Petroleum Engineers Journal*, SPE 9878.
59. Townend, J., Zoback, M.D., 2000. How faulting keeps the crust strong, *Geology*, 28:5, 399-402.

Copyright © MiReCOL Consortium 2014-2017

60. Van den Hoek, P.J., Matsuura, T., De Kroon, M., Gheissary, G., 1999. Simulation of produced water reinjection under fracturing conditions, *SPE Prod. & Facilities* 14 (3), SPE 57385.
61. Vandeweijer, V.P., Groenenberg, R., Donselaar, R., Pluymaekers, M., Loeve, D., Hofstee, C., Nepveu, M., Orlic, B., Akemu, O., Miersemann, U., Benedictus, T., Arts, R., Neele, F., Meindertsma, W., 2011. *Feasibility study P18.* CATO-2 report CATO2-WP3.01-D06.
62. Van Wees, J.D., Buijze, L., Van Thienen-Visser, K., Nepveu, M., Wassing, B.B.T., Orlic, B., Fokker, P.A., 2014. Geomechanics response and induced seiamicity during gas field depletion in the Netherlands, *Geothermics*, http://dx.doi.org/10.1016/j.geothermics.2014.05.004.
63. Vidal-Gilbert, S., Tenthorey, E., Dewhurst, D., Ennis-King, J., Van Ruth, P., Hillis, R., 2010. Geomechanical analysis of the Naylor Field, Otway Basin, Australia: Implications for CO_2 injection and storage, *International Journal of Greenhouse Gas Control*, 4(5), 827-839.
64. Vilarrasa, V., 2014. Impact of CO_2 injection through horizontal and vertical wells on the caprock mechanical stability, *International Journal of Rock Mechanics and Mining Sciences*, 66(0), 151-159.
65. Walsh, S.C., Du Frane, W., Mason, H., Carroll, S., 2013. Permeability of Wellbore-Cement Fractures Following Degradation by Carbonated Brine, *Rock Mechanics and Rock Engineering*, 46(3), 455-464.
66. Warpinski, N.R., Teufel, L.W., 1987. Influence of geological discontinuities on hydraulic fracture propagation, *Journal of Petroleum Technology*, 209-220, SPE 13224.
67. Wibberly, C.A.J., Yielding, G., Di Torro, G., 2008. Recent advances in the understanding of fault zone internal structure: a review, In Wibberly, C.A.J., Kurz, A.J., Imber, J., Holdsworh, R.E., Colletinni, C. (eds), *The Internal Structure o Fault Zones: Implications for Mechanical and Fluid-Flow Properties*, Geological Society of London Special Publication 299, 5-33.
68. Wu, H., Chudnovsky, A., Dudley, J.W., Wong, G.K., 2004. A map of fracture behavior in the vicinity of an interface, Gulf Rocks 2004, Proceedings of the 6th North American Rock Mechanics Symposium, Houston, Texas, June 5-9, ARMA/NARMS 04-620.
69. Yeo, I.W., de Freitas, M.H., Zimmerman, R.W., 1998. Effect of shear displacement on the aperture and permeability of a rock fracture, *International Journal of Rock Mechanics and Mining Sciences*, 35(8), 1051-1070.
70. Yielding, G., 2002. Shale Gouge Ratio – calibration by geohistory, In Koestler, A.G., Hunsdale, R. (eds), *Hydrocarbon Seal Quantification*, NPF Special Publication 11, 1–15, Elsevier Science.
71. Yielding, G., Freeman, B., Needham, D., 1997. Quantitative fault seal prediction, *AAPG Bulletin*, 81:6, 897-917.
72. Zhang, X., Jeffry, R.G., 2004. Hydraulic fracture propagation across frictional interfaces, *US Rock Mechanics / Geomechanics Symposium*, ARMA-07-2004.
73. Zijlstra, E.B., Reemst, P.H.M., Fisher, Q.J., 2007. Incorporation of fault properties into production simulation models of Permian reservoirs from the southern North Sea, In: Jolley, S.J., Barr, D., Walsh, J.J., Knipe, R.J. (eds), *Structurally Complex Reservoirs*, Geological Society, London, Special Publications, 292, 295–308.

Copyright © MiReCOL Consortium 2014-2017

74. Zimmerman, R.W., Kumar, S., Bodvarsson, G.S., 1991. Lubrication theory analysis of the permeability of rough-walled fractures, *International Journal of Rock Mechanics and Mining Sciences & Geomechanics Abstracts*, 28(4), 325-331.
75. Zoback, M.D., 2007. *Reservoir Geomechanics*, Cambridge.
76. Zoback, M., Zinke, J., 2002. Production-induced Normal Faulting in the Valhall and Ekofisk Oil Fields, in *The Mechanism of Induced Seismicity*, edited by C. Trifu, 403-420, Birkhäuser Basel.

Copyright © MiReCOL Consortium 2014-2017